

Fotios Georgiades<sup>1</sup>

## DYNAMICS OF A SPINNING SHAFT WITH NON-CONSTANT ROTATING SPEED, LEADING TO THEOREMS IN MECHANICS

*Abstract.* Recent developments in nonlinear dynamic analysis of mechanical systems are discussed. The nonlinear dynamic analysis of a spinning shaft with non-constant rotating speed, as a specific type of hybrid system, in various ways is done. Due to rigid body angular rotation, this type of hybrid system admits rigid body modes associated with zero eigenvalues. Therefore the Lyapunov approximation of the nonlinear dynamics behaviour with the underlying linear system modes for low energies is not necessarily valid, and the presented two analyses are becoming more valuable. The first analysis is the well-established multiple scales nonlinear dynamic analysis. In the 2<sup>nd</sup> analysis, rigid body motion's backbone curves have been determined and lead to additional information. The nonlinear dynamic analysis of the spinning shaft expanded further, including the new concept of perpetual points, leading to the preliminary conclusion that mechanical system's perpetual points are associated with rigid body motions. Although the nonlinear dynamics analysis of the spinning shaft is extensive in mathematical formulation, a concrete outcome for critical situations is not established yet, and more work is needed.

Moreover, based on the observation for the perpetual points, two theorems proved that the perpetual points are associated with the rigid body motions in linear natural, unforced systems, and they are forming the perpetual manifolds. With some new definitions in mechanics, a third theorem and one corollary proved with the significant outcome the conditions of wave-particle motion of flexible mechanical systems. The presented work is significant in two directions; the first is about examining the dynamics of nonlinear systems with the underlying linear system with zero eigenvalues, associated with mechanical systems with rigid body angular rotations with non-constant rotating

speed. The 2<sup>nd</sup> direction is developing the perpetual mechanic's theory, with the significant 3<sup>rd</sup> theorem in mathematics, physics/mechanics, and mechanical engineering. In mathematics, the theorem provides solutions in non-autonomous N-degrees of freedom systems. In physics/mechanics the particle-wave motion is of high significance. Finally in mechanical engineering the rigid body motion without any oscillation is the ultimate possible type of motion, e.g., trains, cars, etc.

*Mathematics Subject Classification (2010):* Primary: 70-99, 74-99, 70F35, 92C10, 74L10; Secondary: 70Exx, 70KXX, 74M05, 37H20.

*Keywords:* hybrid systems, spinning shaft, perpetual manifolds, perpetual mechanical systems, augmented perpetual manifolds, wave particle motion.

<sup>1</sup> Centre of Perpetual Mechanics & Centre for Nonlinear Systems, Department of Mechanical Engineering, Chennai Institute of Technology, Chennai, India  
fotiosgeorgiades@citchennai.net

## CONTENTS

1.	Introduction	265
2.	Spinning shaft with non-constant rotating speed	266
2.1.	Model of the spinning shaft	266
2.2.	Multiple scales dynamic analysis	270
2.3.	Alternative dynamic analysis through the perpetual points of the system	276
2.4.	Numerical results from theoretical analysis	289
2.5.	Discussion of this section	296
3.	Theorems in mechanics about rigid body motions	297
3.1.	Theorems about perpetual points of mechanical systems	297
3.2.	Definitions of perpetual mechanical systems, augmented perpetual manifolds, and a relevant theorem with a corollary	299
3.3.	Discussion of this section	305
4.	Conclusions	306
	References	306
	Appendix-A	308
A.1	Solution of torsional with rigid body angular motion, equations.	308
A.2	Solution of lateral bending motion equations.	310

## 1. Introduction

This invited review article summarizes the latest research of the author's outcome relevant to the concept of the hybrid systems developed by Prof. K.R. (Stevanovic) Hedrih. The concept of hybrid systems defined in [1], formed by several subsystems, is examined in a hybrid system (particular type), a spinning shaft with non-constant rotating speeds. The rigid body acceleration is a generalized coordinate of the shaft coupled with the elastic deformation generalized coordinates on this system.

Starting from the model of the spinning shaft, then nonlinear dynamic analysis in two ways is presented.

The outcome of applying the very well-established multiple scales analysis developed in [2] up to two-time scales in the spinning shaft dynamics is presented. In the main text, the systems of differential equations describing the motions are shown. The associated solutions, alongside the system of differential equations in the main text, are referenced and in Appendix-A explicitly are shown.

Through a different approach developed in [3], the dynamic analysis of the spinning shaft, by examining particular points relevant to the dynamics of the spinning shaft in two ways, is extended. The first type of points arises by considering a restricting system that describes the motion of the spinning shaft [3]. Chaotic dynamics of the spinning shaft is discussed in [4]. Moreover, to expand the dynamic analysis characteristics, the concept of perpetual points (PPs) is employed. Prasad has defined the PPs in [5], and mainly to identify hidden attractors in, e.g. [6], are used.

Linearization around the fixed points of the restricted system or otherwise stated around the PPS is performed and leads to three different sets describing the motion for different rigid body angular velocities. The eigenvalues of the dynamical systems, determined in [3], are shown. A 3D plot of all the perpetual points with the associated eigenvalues of the linearized dynamical systems is shown. Moreover, using the linearized system's eigenvalues, the normal modes of the spinning shaft, determined in [3], are explained.

The significance of the nonlinear dynamic analyses, with multiple scales and the linearization around the perpetual points of the spinning shaft, are discussed.

The observation that the perpetual points of the spinning shaft are associated with rigid body motions leads to further development of theory relevant to perpetual points as follows. Two theorems about the nature of perpetual points in linear natural mechanical unforced systems stated and proved in [7-8] are presented. Based on these theorems, some new definitions for mechanical systems [9] herein are presented. These definitions lead to the statement of a theorem in [10], which makes the proof very easy in [9]. The theorem herein is presented, and an analytical and numerical example is certified. Before the conclusions, there is a discussion for the already developed theory about the perpetual points.

## 2. Spinning shaft with non-constant rotating speed

A spinning shaft with a non-constant rotating speed, as a hybrid system, is considered. The hybrid system description is in the sense that the rigid body rotation due to not necessarily zero acceleration forms a generalized coordinate coupled with the generalized coordinates that describe the elastic deformation of the shaft.

In §2.1, there is the model of the spinning shaft, and then in the subsequent sections, the nonlinear dynamic analysis with two ways is presented. The multiple scales nonlinear dynamic analysis is in §2.2, and an alternative nonlinear dynamic analysis is in §2.3. The analytical findings in §2.4 with numerical simulations are verified. Finally, in §2.4, there is a summary of the research outcome with future research directions.

**2.1. Model of the spinning shaft.** A flexible shaft with length  $-L$ , made of a material with density  $-\rho$ , Young's (shear) modulus  $-E$  ( $G$ ) and internal (external) diameter  $-D_i$  ( $D_o$ ), is considered. The distributed mass  $-m$  and the inertia coefficient for torsion  $-I_1$  are given by,

$$m = \rho A = \pi \rho \left( \frac{D_o^2 - D_i^2}{4} \right), \quad (1a)$$

$$I_1 = \rho I = \pi \rho \left( \frac{D_o^4 - D_i^4}{64} \right), \quad (1b)$$

whereas  $A$  is the area of the cross section, and  $I$  is the second moment of the area of the cross section of the shaft.

The shaft considered as an Euler-Bernoulli linearly deformed beam with deformation indicated in Figure 1. The lateral bending ( $v$ ,  $w$ ) deformations are

coupled with the torsional ( $\varphi$ ) deformation and the rigid body angular rotation ( $\theta$ ), noting that the axial deformation is fully decoupled from the rest, as in [2] is shown.

A first attempt in modelling a spinning shaft with the non-constant rotating speed was in [11], but there are missing terms in the partial differential equation defining the torsion, and the complete derivation repeated in [2].



FIGURE 1. The configuration of the spinning shaft, with the coupled generalized coordinates of deformations ( $v, w, \varphi$ ), their associated modal generalized coordinates ( $q_v, q_w, q_\varphi$ ), and the associated direction of the angular rigid body coordinate ( $\theta$ ), velocity ( $\dot{\theta}$ ), and acceleration ( $\ddot{\theta}$ ).

The system of equations describing the motion, apart from the partial differential equations (PDEs), includes an integrodifferential equation as shown in [2]. Considering hinged-hinged (fixed position-free rotation) boundary conditions for the lateral bending motions and fixed-free for the torsional motion, PDEs, solve the eigenvalue problem and then using Bubnov-Galerkin approximation, in their first mode shapes are projected [2]. The deformation in torsion ( $\varphi$ ), to the ‘modal’ torsional generalized coordinate  $-q_\varphi$ , is projected, and the lateral bending deformations ( $v, w$ ) are projected to the modal lateral bending generalized coordinates ( $q_v, q_w$ ), and lead to the following system of ‘modal’ equations,

$$\left[1 + \frac{q_v^2}{2 \cdot I_1 \cdot L} + \frac{q_w^2}{2 \cdot I_1 \cdot L} + \frac{q_\phi^2}{I_1 \cdot L}\right] \cdot \ddot{\theta} - \frac{F}{I_1 \cdot L} \cdot \ddot{q}_\phi - \frac{q_v \cdot \ddot{q}_w}{2 \cdot I_1 \cdot L} + \frac{\ddot{q}_v \cdot q_w}{2 \cdot I_1 \cdot L} = -\frac{\dot{\theta} \cdot \dot{q}_v \cdot q_v}{I_1 \cdot L} - \frac{\dot{\theta} \cdot \dot{q}_w \cdot q_w}{I_1 \cdot L} - \frac{2 \cdot \dot{\theta} \cdot \dot{q}_\phi \cdot q_\phi}{I_1 \cdot L} = \frac{h_1}{I_1 \cdot L}, \tag{2a}$$

$$\ddot{\theta} \cdot q_w + (1 - M) \cdot \ddot{q}_v = [\dot{\theta}^2 - \omega_b^2 \cdot (1 - M)] \cdot q_v - 2 \cdot \dot{\theta} \cdot \dot{q}_w = h_2, \tag{2b}$$

$$-\dot{\theta} \cdot q_v + (1 - M) \cdot \ddot{q}_w = [\dot{\theta}^2 - \omega_b^2 \cdot (1 - M)] \cdot q_w + 2 \cdot \dot{\theta} \cdot \dot{q}_v = h_3, \tag{2c}$$

$$-F \cdot \ddot{\theta} + \ddot{q}_\phi = \dot{\theta}^2 \cdot q_\phi - \omega_T^2 \cdot q_\phi = h_4, \tag{2d}$$

whereas, overdot means derivative in time, and the rigid body angular generalized coordinate as  $\theta$  is denoted. Also the constants in equations (2) are given by,

$$F = \frac{2}{\pi} \cdot \sqrt{2 \cdot I_1 \cdot L}, \tag{3a}$$

$$M = -\frac{I_1 \cdot \pi^2}{m \cdot L^2}, \tag{3b}$$

$$\omega_b = \sqrt{\frac{\pi^4 \cdot E \cdot I}{L^2 \cdot \pi^2 \cdot I_1 + L^4 \cdot m}}, \tag{3c}$$

$$\omega_T = \frac{\pi}{2 \cdot L} \cdot \sqrt{\frac{G \cdot I}{I_1}} \tag{3d}$$

The last two formulas correspond to the natural frequencies obtained by solving the PDE's eigenvalue problem of lateral bending motion ( $\omega_b$ ) and torsion ( $\omega_r$ ) for the considered boundary conditions. The shaft angular deformation, by the sum of the rigid body angular position ( $\theta$ ) adding the local torsional deformation ( $\phi$ ), is defined, noting that the actual natural frequency in torsion with free-free boundary conditions must be defined; therefore, is not by the equation (3d), and this is the reason of the punctuation in 'modal' displacements for torsion.

The system of equations (2) can be written in matrix form,

$$\begin{bmatrix} m_t & q_w & -q_v & -2 \cdot F \\ q_w & (1 - M) & 0 & 0 \\ -q_v & 0 & (1 - M) & 0 \\ -F & 0 & 0 & 1 \end{bmatrix} \cdot \begin{Bmatrix} \ddot{\theta} \\ \ddot{q}_v \\ \ddot{q}_w \\ \ddot{q}_\phi \end{Bmatrix} = [M_{tot}] \cdot \begin{Bmatrix} \ddot{\theta} \\ \ddot{q}_v \\ \ddot{q}_w \\ \ddot{q}_\phi \end{Bmatrix} = \begin{Bmatrix} h_1 \\ h_2 \\ h_3 \\ h_4 \end{Bmatrix} \tag{4}$$

with,

$$m_t = 2 \cdot I_1 \cdot L + q_v^2 + q_w^2 + 2 \cdot q_\phi^2 \tag{5}$$

Considering the inverse of inertia matrix, then the equations (4) are taking the form,

$$\{\ddot{\theta} \quad \ddot{q}_v \quad \ddot{q}_w \quad \ddot{q}_\phi\}^T = [M_{tot}]^{-1} \cdot \{h_1 \quad h_2 \quad h_3 \quad h_4\}^T \tag{6}$$

which, is the Cauchy form of differential equations (2). The inverse of the nonsingular inertia matrix is given by,

$$[M_{tot}]^{-1} = \frac{1}{\delta} \cdot \begin{bmatrix} (1 - M) & -q_w & q_v & 2 \cdot (1 - M) \cdot F \\ -q_w & m_t - \frac{q_v^2}{(1 - M)} - 2 \cdot F^2 & -\frac{q_v \cdot q_w}{(1 - M)} & -2 \cdot F \cdot q_w \\ q_v & -\frac{q_v \cdot q_w}{(1 - M)} & m_t - \frac{q_w^2}{(1 - M)} - 2 \cdot F^2 & 2 \cdot F \cdot q_v \\ F \cdot (1 - M) & -F \cdot q_w & F q_v & (1 - M) \cdot m_t - q_v^2 - q_w^2 \end{bmatrix} \tag{7a}$$

$$\delta = 2(1 - M)(I_1 L - F^2) - M q_v^2 - M q_w^2 + 2(1 - M) q_\phi^2 > 0, \tag{7b}$$

Some observations of the above systems eqs. (4), (6) are necessary before presenting any nonlinear dynamic analysis of the equations (2) or (4). Considering the following change of variables [3,12],

$$\begin{aligned} \{x_1 \quad x_2 \quad x_3 \quad x_4 \quad x_5 \quad x_6 \quad x_7 \quad x_8\}^T &= \\ &= \{\theta \quad q_v \quad q_w \quad q_\phi \quad \dot{\theta} \quad \dot{q}_v \quad \dot{q}_w \quad \dot{q}_\phi\}^T, \end{aligned} \tag{8}$$

the system of equations (2) or (4), (6) can be written as 1<sup>st</sup> order dynamical system with the following form [3,12],

$$\{\dot{x}_i\} = [C] \times \{x_i\} + \frac{1}{\delta} \cdot [0,0,0,0, G_1, G_2, G_3, G_4]^T, \tag{9}$$

with,

$$[\mathbf{C}] = \begin{bmatrix} 0 & 0 & 0 & 0 & 1 & 0 & 0 & 0 \\ 0 & 0 & 0 & 0 & 0 & 1 & 0 & 0 \\ 0 & 0 & 0 & 0 & 0 & 0 & 1 & 0 \\ 0 & 0 & 0 & 0 & 0 & 0 & 0 & 1 \\ 0 & 0 & 0 & 0 & 0 & 0 & 0 & 0 \\ 0 & 0 & 0 & 0 & 0 & 0 & 0 & 0 \\ 0 & 0 & 0 & 0 & 0 & 0 & 0 & 0 \\ 0 & 0 & 0 & 0 & 0 & 0 & 0 & 0 \end{bmatrix}, \quad (10a)$$

and,

$$G_1 = 2 \cdot M \cdot x_2 \cdot x_5 \cdot x_6 + 2 \cdot M \cdot x_3 \cdot x_5 \cdot x_7 - 4 \cdot (1 - M) \cdot x_4 \cdot x_5 \cdot x_8 + \\ + 2 \cdot F \cdot (1 - M) \cdot x_5^2 \cdot x_4 - 2 \cdot F \cdot (1 - M) \cdot \omega_T^2 \cdot x_4, \quad (10b)$$

$$G_2 = -\frac{2 \cdot M}{(1 - M)} \cdot x_2 \cdot x_3 \cdot x_5 \cdot x_6 + 4 \cdot x_3 \cdot x_4 \cdot x_5 \cdot x_8 + 2 \cdot (I_1 \cdot L - F^2) \cdot x_2 \cdot x_5^2 - \\ - \frac{M}{(1 - M)} \cdot x_2^3 \cdot x_5^2 - \frac{M}{(1 - M)} \cdot x_2 \cdot x_3^2 \cdot x_5^2 + 2 \cdot x_2 \cdot x_4^2 \cdot x_5^2 - \\ - 2 \cdot \omega_b^2 \cdot (1 - M) \cdot (I_1 \cdot L - F^2) \cdot x_2 + \frac{M \cdot \omega_b^2 \cdot (1 - M)}{(1 - M)} \cdot x_2^3 + \\ + \frac{\omega_b^2 \cdot M \cdot (1 - M)}{(1 - M)} \cdot x_2 \cdot x_3^2 - 2 \cdot \omega_b^2 \cdot (1 - M) \cdot x_4^2 \cdot x_2 - 4 \cdot (I_1 \cdot L - F^2) \cdot x_5 \cdot x_7 + \\ + \frac{2 \cdot M}{(1 - M)} \cdot x_2^2 \cdot x_5 \cdot x_7 - 4 \cdot x_5 \cdot x_7 \cdot x_4^2 - 2 \cdot F \cdot (y_4^2 - \omega_T^2) \cdot x_3 \cdot x_4, \quad (10c)$$

$$G_3 = \frac{2 \cdot M}{(1 - M)} \cdot x_2 \cdot x_3 \cdot x_5 \cdot x_7 - 4 \cdot x_2 \cdot x_4 \cdot x_5 \cdot x_8 - \\ - 2 \cdot (I_1 \cdot L - F^2) \cdot \omega_b^2 \cdot (1 - M) \cdot x_3 + \omega_b^2 \cdot M \cdot x_2^2 \cdot x_3 + \omega_b^2 \cdot M \cdot x_3^3 - \\ - 2 \cdot \omega_b^2 \cdot (1 - M) \cdot x_3 \cdot x_4^2 + 2 \cdot (I_1 \cdot L - F^2) \cdot x_3 \cdot x_5^2 - \frac{M}{(1 - M)} \cdot x_2^2 \cdot x_3 \cdot x_5^2 - \\ - \frac{M}{(1 - M)} \cdot x_3^3 \cdot x_5^2 + 2 \cdot x_3 \cdot x_4^2 \cdot x_5^2 + 4 \cdot (I_1 \cdot L - F^2) \cdot x_5 \cdot x_6 - \\ - \frac{2 \cdot M}{(1 - M)} \cdot x_3^2 \cdot x_5 \cdot x_6 + 4 \cdot x_4^2 \cdot x_5 \cdot x_6 + 2 \cdot F \cdot x_2 \cdot x_4 \cdot x_5^2 - \\ - 2 \cdot F \cdot \omega_T^2 \cdot x_2 \cdot x_4, \quad (10d)$$

$$G_4 = 2 \cdot F \cdot M \cdot x_2 \cdot x_5 \cdot x_6 + 2 \cdot F \cdot M \cdot x_3 \cdot x_5 \cdot x_7 - 4 \cdot F \cdot (1 - M) \cdot x_4 \cdot x_5 \cdot x_8 + \\ + 2 \cdot (1 - M) \cdot I_1 \cdot L \cdot x_4 \cdot x_5^2 - M \cdot x_2^2 \cdot x_4 \cdot x_5^2 - M \cdot x_3^2 \cdot x_4 \cdot x_5^2 + \\ + 2 \cdot (1 - M) \cdot x_4^3 \cdot x_5^2 - 2 \cdot (1 - M) \cdot I_1 \cdot L \cdot \omega_T^2 \cdot x_4 + M \cdot \omega_T^2 \cdot x_2^2 \cdot x_4 + \\ + M \cdot \omega_T^2 \cdot x_3^2 \cdot x_4 - 2 \cdot (1 - M) \cdot \omega_T^2 \cdot x_4^3. \quad (10e)$$

The first term in the right-hand side of equation (9) is the linear term of the system, and examining the explicit form of the matrix  $-\mathbf{[C]}$  given by equation (10a) is easy to find out that it has many zero eigenvalues, which means that the Lyapunov linear modes approximation of the nonlinear system in small energies is not necessarily valid [12]. Therefore the linearized approximation of the nonlinear system cannot

help much in obtaining nonlinear solutions. All the methods relying on the natural frequencies of the underlying linear system developed for this nonlinear system will not necessarily lead to a good approximation of the original system.

In the following two sections, two different methods for the nonlinear dynamic analysis of the shaft identifying critical situations developed in [2-3,12], are explained. More precisely, the multiple scales nonlinear dynamic analysis developed in [2]; and linearization around the equilibrium manifolds of a restricted system or otherwise stated through the linearization around the system's (4) perpetual manifolds are shown.

**2.2. Multiple scales dynamic analysis.** The multiple scales perturbation method, developed by Nayfeh in [13], used for the nonlinear dynamic analysis of the spinning shaft in [2], in this section is presented.

This method is based on the dynamic analysis of the nonlinear differential equations, with different time scales  $-T_i$  as follows,

$$T_j = \varepsilon^j \cdot t, \quad (11a)$$

therefore, the derivatives are given by,

$$\frac{d}{dt} = \sum_{k=0}^{\infty} \varepsilon^k \cdot D_k, \quad (11b)$$

whereas  $D_k$  indicates the derivative in  $T_k$  - time scale.

The accelerations are given by,

$$\frac{d^2}{dt^2} = \sum_{j=0}^{\infty} \sum_{k=0}^{\infty} \varepsilon^{k+j} \cdot D_k D_j. \quad (11c)$$

The multiple scales approach leads to the solutions of the 'modal' equations system eq. (2) in the following form,

$$\theta = \varepsilon^0 \cdot \theta_0 + \varepsilon^1 \cdot \theta_1 + \varepsilon^2 \cdot \theta_2 + HOT, \quad (12a)$$

$$q_v = \varepsilon^1 \cdot q_{v,1} + \varepsilon^2 \cdot q_{v,2} + HOT, \quad (12b)$$

$$q_w = \varepsilon^1 \cdot q_{w,1} + \varepsilon^2 \cdot q_{w,2} + HOT, \quad (12c)$$

$$q_\phi = \varepsilon^1 \cdot q_{\phi,1} + \varepsilon^2 \cdot q_{\phi,2} + HOT. \quad (12d)$$

Also, following the multiple scales approach, the system of equations (2) for the various  $\varepsilon$ -scale orders (up to the 2<sup>nd</sup> order) is taking the form:

$$\varepsilon^0, D_0^2 \theta_0 = 0 \Leftrightarrow D_0 \theta_0 = \Omega \Leftrightarrow \theta_0 = \Omega \cdot T_0 + ct, \quad (13)$$

$$\varepsilon^1, 2 \cdot I_1 \cdot L \cdot D_0^2 \theta_1 - 2 \cdot F \cdot D_0^2 q_{\phi,1} = -4 \cdot I_1 \cdot L \cdot D_0 D_1 \theta_0, \quad (14a)$$

$$D_0^2 \theta_0 \cdot q_{w,1} + (1 - M) \cdot D_0^2 q_{v,1} - (D_0 \theta_0)^2 \cdot q_{v,1} + \omega_b^2 \cdot (1 - M) \cdot q_{v,1} + 2 \cdot D_0 \theta_0 \cdot D_0 q_{w,1} = 0, \quad (14b)$$

$$-D_0^2 \theta_0 \cdot q_{v,1} + (1 - M) \cdot D_0^2 q_{w,1} - (D_0 \theta_0)^2 \cdot q_{w,1} + \omega_b^2 \cdot (1 - M) \cdot q_{w,1} - 2 \cdot D_0 \theta_0 \cdot D_0 q_{v,1} = 0, \quad (14c)$$

$$-F \cdot D_0^2 \theta_1 + D_0^2 q_{\phi,1} - (D_0 \theta_0)^2 \cdot q_{\phi,1} + \omega_T^2 \cdot q_{\phi,1} = 2 \cdot F \cdot D_0 D_1 \theta_0, \quad (14d)$$

$$\begin{aligned} \varepsilon^2, \quad & 2 \cdot I_1 \cdot L \cdot D_0^2 \theta_2 - 2 \cdot F \cdot D_0^2 q_{\phi,2} = F_1 = \\ & = -2 \cdot I_1 \cdot L \cdot (2 \cdot D_0 D_1 \theta_1 + 2 \cdot D_0 D_2 \theta_0 + D_1^2 \theta_0) - D_0^2 \theta_0 \cdot q_{v,1}^2 - D_0^2 \theta_0 \cdot q_{w,1}^2 - \\ & - 2 \cdot D_0^2 \theta_0 \cdot q_{\phi,1}^2 + 4 \cdot F \cdot D_0 D_1 q_{\phi,1} + q_{v,1} \cdot D_0^2 q_{w,1} - q_{w,1} \cdot D_0^2 q_{v,1} - \\ & - 2 \cdot D_0 \theta_0 \cdot D_0 q_{v,1} \cdot q_{v,1} - 2 \cdot D_0 \theta_0 \cdot D_0 q_{w,1} \cdot q_{w,1} - 4 \cdot D_0 \theta_0 \cdot D_0 q_{\phi,1} \cdot q_{\phi,1}, \quad (15a) \end{aligned}$$

$$\begin{aligned} & D_0^2 \theta_0 \cdot q_{w,2} + (1 - M) \cdot D_0^2 q_{v,2} - (D_0 \theta_0)^2 \cdot q_{v,2} + \omega_b^2 \cdot (1 - M) \cdot q_{v,2} + \\ & + 2 \cdot D_0 \theta_0 \cdot D_0 q_{w,2} = F_2 = -D_0^2 \theta_1 \cdot q_{w,1} - 2 \cdot D_0 D_1 \theta_0 \cdot q_{w,1} - \\ & - 2 \cdot (1 - M) \cdot D_0 D_1 q_{v,1} + 2 \cdot D_0 \theta_0 \cdot D_0 \theta_1 \cdot q_{v,1} + 2 \cdot D_0 \theta_0 \cdot D_1 \theta_0 \cdot q_{v,1} - \\ & - 2 \cdot D_0 \theta_0 \cdot D_1 q_{w,1} - 2 \cdot D_0 \theta_1 \cdot D_0 q_{w,1} - 2 \cdot D_1 \theta_0 \cdot D_0 q_{w,1}, \quad (15b) \end{aligned}$$

$$\begin{aligned} & -D_0^2 \theta_0 \cdot q_{v,2} + (1 - M) \cdot D_0^2 q_{w,2} - (D_0 \theta_0)^2 \cdot q_{w,2} + \omega_b^2 \cdot (1 - M) \cdot q_{w,2} - \\ & - 2 \cdot D_0 \theta_0 \cdot D_0 q_{v,2} = F_3 = D_0^2 \theta_1 \cdot q_{v,1} + 2 \cdot D_0 D_1 \theta_0 \cdot q_{v,1} - 2 \cdot (1 - M) \cdot D_0 D_1 q_{w,1} + \\ & + 2 \cdot D_0 \theta_0 \cdot D_0 \theta_1 \cdot q_{w,1} + 2 \cdot D_0 \theta_0 \cdot D_1 \theta_0 \cdot q_{w,1} + \\ & + 2 \cdot D_0 \theta_0 \cdot D_1 q_{v,1} + 2 \cdot D_0 \theta_1 \cdot D_0 q_{v,1} + 2 \cdot D_1 \theta_0 \cdot D_0 q_{v,1}, \quad (15c) \end{aligned}$$

$$\begin{aligned} & -F \cdot D_0^2 \theta_2 + D_0^2 q_{\phi,2} - (D_0 \theta_0)^2 \cdot q_{\phi,2} + \omega_T^2 \cdot q_{\phi,2} = F_4 = F \cdot (2 \cdot D_0 D_1 \theta_1 + \\ & + 2 \cdot D_0 D_2 \theta_0 + D_1^2 \theta_0) - 2 \cdot D_0 D_1 q_{\phi,1} + 2 \cdot D_0 \theta_0 \cdot D_0 \theta_1 \cdot q_{\phi,1} + \\ & + 2 \cdot D_0 \theta_0 \cdot D_1 \theta_0 \cdot q_{\phi,1}. \quad (15d) \end{aligned}$$

Eliminating secular terms in equation (14a) and considering equation (13) leads to [2],

$$D_0 D_1 \theta_0 = 0 \Leftrightarrow D_1 \Omega = 0 \Leftrightarrow D_1 \Omega \cdot T_0 = D_1 \theta_0 = 0. \quad (16)$$

The equation (16) provides a very helpful expression to eliminate the other secular terms in equations (14)-(15).

The expressions simplified with the over-dot notation *instead of*  $D_0$  and the dash notation *instead of*  $D_1$ , in the following sections.

On the left side of the equations (14)-(15), the coupled equations in pairs. The first pair of equations describes the rigid body angular position with torsional ‘modal’ displacement, and the second pair comprised of the two equations describing the lateral bending modal displacements. Therefore the multiple scales nonlinear dynamic analysis of the spinning shaft is divided into two analyses. The 1st one is about the dynamics of the spinning shaft in rotation, which involves rigid body angular and torsional motion presented in the following subsection. The 2<sup>nd</sup> analysis is related to lateral bending motions that are presented just after the following subsection.

**Multiple scales analysis, the equations describing torsional with rigid body angular motions.** In this subsection, the systems of equations of motion describing the dynamics of torsional with rigid body motion at different scales are shown, with referenced their solutions that in Appendix-A, are explicitly shown. More precisely, the multiple scales dynamic analysis in this section involves the solution of the 1<sup>st</sup>

order approximation, without and with amplitude modulations, and the 2<sup>nd</sup> order approximation without amplitude modulation.

*The 1<sup>st</sup> order approximation system describing torsional motion*

The 1<sup>st</sup> order approximation equations describing torsional with rigid body angular motions in  $T_0$ - time scale by equations (14a,d) are obtained [2], and they are given by,

$$2 \cdot I_1 \cdot L \cdot \ddot{\theta}_1 - 2 \cdot F \cdot \ddot{q}_{\phi,1} = 0 \Leftrightarrow \ddot{\theta}_1 = \frac{F}{I_1 \cdot L} \cdot \ddot{q}_{\phi,1}, \quad (17a)$$

$$-F \cdot \ddot{\theta}_1 + \ddot{q}_{\phi,1} + (\omega_T^2 - \Omega^2) \cdot q_{\phi,1} = 0 \Leftrightarrow \ddot{q}_{\phi,1} + \frac{I_1 \cdot L \cdot (\omega_T^2 - \Omega^2)}{(I_1 \cdot L - F^2)} \cdot q_{\phi,1} = 0. \quad (17b)$$

The solution of this system, obtained in [2], by the equations (A.1a-b) in Appendix-A, is given. The natural frequency  $-\mu_0$  by the equation (A.2) is defined.

In case that the rigid body angular velocity ( $\Omega$ ) is equal to the 'torsional frequency' ( $\omega_T$ ), then the oscillatory frequency ( $\mu_0$ ) in equations (A.1a-b) becomes zero.

*The amplitude modulation equations of the 1<sup>st</sup> order approximation describing torsional motion*

The amplitude modulation equations by the  $T_1$ - time scale arise, with the elimination of the secular terms in equations (15a,d) [2], and they are given by:

$$A'_{\phi,1} = -\mu_1 \cdot A_{\phi,2}, \quad (18a)$$

$$A'_{\phi,2} = \mu_1 \cdot A_{\phi,1}. \quad (18b)$$

The solution of equations (18a-b) defines the modulation amplitudes, and their explicit form obtained in [2] by the equations (A.6a-d) in Appendix-A is given. The overall 1<sup>st</sup> order approximation solution, also considering the amplitude modulation, by the equations (A.8a-b) of Appendix-A, is given. The detuning frequency ( $\mu_1$ ) by the equation (A.6) is given. The detuning frequency is not defined whenever the rigid body angular velocity is equal to the torsional frequency  $-\mu_0$  since the torsional frequency is a denominator, and in these cases, becomes zero.

*The 2<sup>nd</sup> order approximation system describing torsional motion*

The system of equations describing the 2<sup>nd</sup> order approximations describing the motion in  $T_0$ - time scale by the equations (15a,d) are obtained [2], and they are given by:

$$\ddot{\theta}_2 = S_0 \cdot q_{\phi,2} + [S_1(T_1) \cdot e^{i \cdot 2 \cdot \mu_0 \cdot T_0} + S_2(T_1) \cdot e^{i \cdot 2 \cdot \omega_1 \cdot T_0} + S_3(T_1) \cdot e^{i \cdot 2 \cdot \omega_2 \cdot T_0} + S_4(T_1) \cdot e^{i \cdot (\omega_1 + \omega_2) \cdot T_0} + S_5(T_1) \cdot e^{i \cdot (\omega_1 - \omega_2) \cdot T_0} + cc], \quad (19a)$$

$$\ddot{q}_{\phi,2} + \mu_0^2 \cdot q_{\phi,2} = V_1(T_1) \cdot e^{i \cdot 2 \cdot \mu_0 \cdot T_0} + V_2(T_1) \cdot e^{i \cdot 2 \cdot \omega_1 \cdot T_0} + V_3(T_1) \cdot e^{i \cdot 2 \cdot \omega_2 \cdot T_0} + V_4(T_1) \cdot e^{i \cdot (\omega_1 + \omega_2) \cdot T_0} + V_5(T_1) \cdot e^{i \cdot (\omega_1 - \omega_2) \cdot T_0} + cc, \quad (19b)$$

whereas cc means complex conjugate, and also,

$$S_0 = \frac{-F \cdot \mu_0^2}{I_1 \cdot L}, \quad (20a)$$

$$S_1(T_1) = \frac{F_{1,1}(T_1) + 2 \cdot F \cdot F_{4,1}(T_1)}{2 \cdot (I_1 \cdot L - F^2)}, \quad (20b)$$

$$S_j(T_1) = \frac{F_{1,j}(T_1)}{2 \cdot (I_1 \cdot L - F^2)}, \text{ with } j=2:5, \quad (20c)$$

$$V_1(T_1) = \frac{F \cdot F_{1,1}(T_1) + 2 \cdot I_1 \cdot L \cdot F_{4,1}(T_1)}{2 \cdot (I_1 \cdot L - F^2)}, \quad (20d)$$

$$V_j(T_1) = \frac{F \cdot F_{1,j}(T_1)}{2 \cdot (I_1 \cdot L - F^2)}, \quad \text{with } j=2:5, \quad (20e)$$

with,

$$F_{1,1}(T_1) = -4 \cdot \Omega \cdot \mu_0 \cdot i \cdot A_{22}^2(T_1), \quad (21a)$$

$$F_{1,2}(T_1) = -2 \cdot \Omega \cdot \omega_1 \cdot i \cdot [C_{v1}^2(T_1) + C_{w1}^2(T_1)], \quad (21b)$$

$$F_{1,3}(T_1) = -2 \cdot \Omega \cdot \omega_2 \cdot i \cdot [D_{v1}^2(T_1) + D_{w1}^2(T_1)], \quad (21c)$$

$$F_{1,4}(T_1) = (\omega_1^2 - \omega_2^2) \cdot [C_{v1}(T_1) \cdot D_{w1}(T_1) - C_{w1}(T_1) \cdot D_{v1}(T_1)] - \\ - 2 \cdot \Omega \cdot i \cdot (\omega_1 + \omega_2) \cdot [C_{v1}(T_1) \cdot \underline{D}_{v1}(T_1) + C_{w1}(T_1) \cdot \underline{D}_{w1}(T_1)], \quad (21d)$$

$$F_{1,5}(T_1) = (\omega_1^2 - \omega_2^2) \cdot [C_{v1}(T_1) \cdot \bar{D}_{w1}(T_1) - C_{w1}(T_1) \cdot \bar{D}_{v1}(T_1)] - \\ - 2 \cdot \Omega \cdot i \cdot (\omega_1 - \omega_2) \cdot [C_{v1}(T_1) \cdot \bar{D}_{v1}(T_1) + C_{w1}(T_1) \cdot \bar{D}_{w1}(T_1)], \quad (21e)$$

$$F_{4,1}(T_1) = 2 \cdot \Omega \cdot A_{11}(T_1) \cdot A_{22}(T_1). \quad (21f)$$

The solution is obtained in [2] and in equations (A.9, A.11) of Appendix-A is explicitly defined.

### Multiple scales analysis, the equations describing the lateral bending motions.

In this subsection, the systems of equations of motion describing the dynamics of the two lateral bending motions at different scales are shown, with referenced solutions. The multiple scales dynamic analysis in this section, consistent with the previous subsection dynamic analysis, involves the solution of the 1st order approximation, without and with amplitude modulations, and the 2nd order approximation without amplitude modulation.

#### *The 1<sup>st</sup> order approximation system describing lateral bending motions*

The 1<sup>st</sup> order approximation equations that describe lateral bending motion in  $T_0$ -time scale arise by equations (14b,c) [2], and given by:

$$(1 - M) \cdot \ddot{q}_{v,1} + [\omega_b^2 \cdot (1 - M) - \Omega^2] \cdot q_{v,1} + 2 \cdot \Omega \cdot \dot{q}_{w,1} = 0, \quad (22a)$$

$$(1 - M) \cdot \ddot{q}_{w,1} + [\omega_b^2 \cdot (1 - M) - \Omega^2] \cdot q_{w,1} - 2 \cdot \Omega \cdot \dot{q}_{v,1} = 0. \quad (22b)$$

These equations coincide with those obtained when constant parameter angular velocity is considered, which are the well-known equations examined in the literature for steady states to obtain the Campbell diagram. Considering most of the shaft's configurations that their geometry obeys the ratio given by equation A.14b, and also for low rotating speeds the inequality (A.14d) is valid, then the eigenvalues of the system of equations (22a-b) are pure imaginary, and by the equations (A.17a-d) are given. As mentioned in [2], not all these natural frequencies lead to normal modes since the periodicity conditions must be fulfilled and the following equation,

$$\theta_0(T_{0,T}) - \theta_{0,0} = 0 = \text{mod} [\Omega \cdot T_{0,T}, 2 \cdot \pi] = \text{mod} \left[ \frac{2 \cdot \pi \cdot \Omega}{\omega_{1,2}}, 2 \cdot \pi \right] = 0, \quad (23)$$

is required, which is valid only for  $\omega_i = n\Omega$  (with  $n$  any integer), which leads to the

shaft's critical speeds in steady states, and also defines the shaft's normal modes. For purely imaginary eigenvalues, the equation's solution of (22a-b) by the equations (A.20a-d) is given.

*The amplitude modulation equations of the 1<sup>st</sup> order approximation describing lateral bending motions*

The amplitude modulation equations of the 1<sup>st</sup> order approximation in lateral bending motions by the  $T_1$ -time scale arise, with elimination of the secular terms in equations (15b,c), and they are defined by:

$$\begin{bmatrix} (1-M) \cdot \omega_j & 0 & 0 & -\Omega \\ 0 & -(1-M) \cdot \omega_j & -\Omega & 0 \\ 0 & \Omega & (1-M) \cdot \omega_j & 0 \\ \Omega & 0 & 0 & -(1-M) \cdot \omega_j \end{bmatrix} \cdot \begin{Bmatrix} B_{v2,j}(T_1) \\ B_{v1,j}(T_1) \\ B_{w2,j}(T_1) \\ B_{w1,j}(T_1) \end{Bmatrix} + \begin{bmatrix} 0 & \Omega \cdot A_{11} \cdot A_{11} \cdot \omega_j & -\Omega \\ \Omega \cdot A_{11} & 0 & 0 & -A_{11} \cdot \omega_j \\ -A_{11} \cdot \omega_j & 0 & 0 & \Omega \cdot A_{11} \\ 0 & A_{11} \cdot \omega_j \cdot \Omega \cdot A_{11} & 0 \end{bmatrix} \cdot \begin{Bmatrix} B_{v2,j}(T_1) \\ B_{v1,j}(T_1) \\ B_{w2,j}(T_1) \\ B_{w1,j}(T_1) \end{Bmatrix} = \begin{Bmatrix} 0 \\ 0 \\ 0 \\ 0 \end{Bmatrix}, \quad j = 1, 2, \quad (24)$$

where as,  $j=1$  corresponds to the system arising from first frequency ( $\omega_1$ ) and  $j=2$  to the system arising from the second frequency ( $\omega_2$ ). Considering the detuning frequencies arising by the amplitude modulation equations (24), only the left side of equation (23) defines the critical speeds, and the explicit expression of periodicity becomes very complicated. The system of equations (24) is becoming singular for,

$$(1 - M)\omega_j - \Omega = 0, \quad (25)$$

corresponding to angular velocity very close to the 'critical speed' of the shaft defined by considering the equations (22a,b) and describing the spinning shaft dynamics for constant rotating speed. In case of neglecting rotary inertia terms ( $M = 0$ ), then the system of equations (24) becomes singular for angular velocity on the 'critical speed' of the shaft with dynamics described only by equations (22a,b).

The solution of equations (24), obtained in [2], by equations (A.24a-d) in Appendix-A, explicitly are provided. The detuning frequencies by the equations (A.23a-d) are defined. In the angular velocity on the 'critical speed' of the 1<sup>st</sup> order approximation defined by the equations (22a,b), two of the detuning frequencies given by the equations (A.23a,c) cannot be defined since these equations are becoming singular.

The total solution, arising with the combination of the 1<sup>st</sup> order approximation solution with the detuning frequencies from the amplitude modulation, in Appendix-A by the equations (A.27a-b) is given.

*The 2<sup>nd</sup> order approximation system describing lateral bending motions*

The 2<sup>nd</sup> order approximation equations describing the lateral bending motion in  $T_0$ -time scale [2] obtained by considering equations (15a,b), and they are given by:

$$(1 - M) \cdot \ddot{q}_{v,2} - \Omega^2 \cdot q_{v,2} + \omega_b^2 \cdot (1 - M) \cdot q_{v,2} + 2 \cdot \Omega \cdot \dot{q}_{w,2} = F_2 =$$

$$\begin{aligned}
&= F_{2,1}(T_1) \cdot e^{i(\mu_0+\omega_1)T_0} + F_{2,2}(T_1) \cdot e^{i(\mu_0+\omega_2)T_0} + F_{2,3}(T_1) \cdot e^{i(\mu_0-\omega_1)T_0} + \\
&+ F_{2,4}(T_1) \cdot e^{i(\mu_0-\omega_2)T_0} + cc, \tag{26a}
\end{aligned}$$

$$\begin{aligned}
(1-M) \cdot \ddot{q}_{w,2} - \Omega^2 \cdot q_{w,2} + \omega_b^2 \cdot (1-M) \cdot q_{w,2} - 2 \cdot \Omega \cdot \dot{q}_{v,2} &= F_3 = \\
&= F_{3,1}(T_1) \cdot e^{i(\mu_0+\omega_1)T_0} + F_{3,2}(T_1) \cdot e^{i(\mu_0+\omega_2)T_0} + F_{3,3}(T_1) \cdot e^{i(\mu_0-\omega_1)T_0} + \\
&+ F_{3,4}(T_1) \cdot e^{i(\mu_0-\omega_2)T_0} + cc, \tag{26b}
\end{aligned}$$

with,

$$F_{2,1}(T_1) = A_{12}(T_1) \cdot (-i \cdot \mu_0 \cdot C_{w1}(T_1) + 2 \cdot \Omega \cdot C_{v1}(T_1) - 2 \cdot i \cdot \omega_1 \cdot C_{w1}(T_1)), \tag{27a}$$

$$F_{2,2}(T_1) = A_{12}(T_1) \cdot (-i \cdot \mu_0 \cdot D_{w1}(T_1) + 2 \cdot \Omega \cdot D_{v1}(T_1) - 2 \cdot i \cdot \omega_2 \cdot D_{w1}(T_1)), \tag{27b}$$

$$F_{2,3}(T_1) = A_{12}(T_1) \cdot (-i \cdot \mu_0 \cdot \bar{C}_{w1}(T_1) + 2 \cdot \Omega \cdot \bar{C}_{v1}(T_1) + 2 \cdot i \cdot \omega_1 \cdot \bar{C}_{w1}(T_1)), \tag{27c}$$

$$F_{2,4}(T_1) = A_{12}(T_1) \cdot (-i \cdot \mu_0 \cdot \bar{D}_{w1}(T_1) + 2 \cdot \Omega \cdot \bar{D}_{v1}(T_1) + 2 \cdot i \cdot \omega_2 \cdot \bar{D}_{w1}(T_1)), \tag{27d}$$

$$F_{3,1}(T_1) = A_{12}(T_1) \cdot (i \cdot \mu_0 \cdot C_{v1}(T_1) + 2 \cdot \Omega \cdot C_{w1}(T_1) + 2 \cdot i \cdot \omega_1 \cdot C_{v1}(T_1)), \tag{27e}$$

$$F_{3,2}(T_1) = A_{12}(T_1) \cdot (i \cdot \mu_0 \cdot D_{v1}(T_1) + 2 \cdot \Omega \cdot D_{w1}(T_1) + 2 \cdot i \cdot \omega_2 \cdot D_{v1}(T_1)), \tag{27f}$$

$$F_{3,3}(T_1) = A_{12}(T_1) \cdot (i \cdot \mu_0 \cdot \bar{C}_{v1}(T_1) + 2 \cdot \Omega \cdot \bar{C}_{w1}(T_1) - 2 \cdot i \cdot \omega_1 \cdot \bar{C}_{v1}(T_1)), \tag{27g}$$

$$F_{3,4}(T_1) = A_{12}(T_1) \cdot (i \cdot \mu_0 \cdot \bar{D}_{v1}(T_1) + 2 \cdot \Omega \cdot \bar{D}_{w1}(T_1) - 2 \cdot i \cdot \omega_2 \cdot \bar{D}_{v1}(T_1)), \tag{27h}$$

whereas it is profound that the right-hand side of equations (26a,b) defined by the terms given by equations (27) are becoming zero for,

$$A_{12}(T_1) = 0, \tag{28}$$

or otherwise stated by considering the equations (A.5c-d) with the equation (A.4b), this happens for zero initial conditions of torsional initial 'modal' amplitude and velocity.

The solution of the system of equations (26a-b) in [2] is derived, and by the equations (A.28a-b) is given.

All the individual solutions of the systems of differential equations given in Appendix-A, in [2] numerically, are verified.

In [2], the explicit equations defining the periodicity conditions had not obtained. However, for a shaft with explicitly defined configuration, they can be obtained through the extended Campbell diagram defined by using the plot of the 1<sup>st</sup> order approximation frequencies adding the detuning frequencies plotted with respect to the rigid body angular velocity and the points that a line with slope one is crossing the frequencies curve are the points with critical speed velocity and corresponds to the normal modes of the system.

**2.3. Alternative dynamic analysis through the perpetual points of the system.** In this section, a different approach for nonlinear dynamic analysis is presented. Initially, the equations of a restricted system describing the motion of the spinning shaft and the equations defining the perpetual points of the dynamical system describing the motion of the spinning shaft are presented. Then the fixed points of the restricted system and the perpetual points of the system describing the dynamics of the spinning shaft are shown, and they form the backbone lines of rigid body modes of the spinning shaft. Linearization of the spinning shaft motion equations around the perpetual points in the next subsection is presented, and the eigenvalues of the linearized dynamical systems are shown. Then in the following subsection, the backbone lines of the rigid body modes, incorporating the eigenvalues of the linearized systems around the PPs, for a discussion are presented. In the last subsection, there are the normal modes of the spinning shaft obtained from linearization around the PPs.

**Determination of the perpetual points and the fixed points of a restricted system.** The determination of the fixed points of a restricted system, and the original system's (4), (6) perpetual points, are defined on this subsection. Initially, the equations of the restricted system are presented, then the equations defining the PPs, and finally, the fixed points of the restricted system and the PPs are shown.

*Equations of the restricted system*

In [3], recognizing that the rigid body angular position ( $x_1 = \theta$ ) is not involved explicitly in any of the equations (4), (6), without losing any information, it can be neglected by using the following change of variables,

$$\{y_1 \ y_2 \ y_3 \ y_4 \ y_5 \ y_6 \ y_7\}^T = \{q_v \ q_w \ q_\phi \ \dot{\theta} \ \dot{q}_v \ \dot{q}_w \ \dot{q}_\phi\}^T, \quad (29)$$

which leads to the following 1<sup>st</sup> order restricted system of differential equations that describes the motion,

$$\dot{y}_1 = y_5, \quad (30a)$$

$$\dot{y}_2 = y_6, \quad (30b)$$

$$\dot{y}_3 = y_7, \quad (30c)$$

$$\{\dot{y}_4 \ \dot{y}_5 \ \dot{y}_6 \ \dot{y}_7\}^T = \frac{1}{\delta} \cdot \{F_1 \ F_2 \ F_3 \ F_4\}^T. \quad (30d)$$

Since the equation describing the motion is decoupled from the equations (30), the rigid body angular displacement can be easily determined with the direct integration of the expression defining the rigid body angular velocity ( $y_4 = \dot{\theta}$ ).

The explicit form of the right-hand side of the vector field in equation (30d) arise by using the explicit form of the multiplication of the inverse of the inertia matrix with the vector, using the above change of variables (eq. 29), and is given by [3],

$$\begin{aligned} F_1 &= 2 \cdot M \cdot y_1 \cdot y_4 \cdot y_5 + 2 \cdot M \cdot y_2 \cdot y_4 \cdot y_6 - 4 \cdot (1 - M) \cdot y_3 \cdot y_4 \cdot y_7 + \\ &+ 2 \cdot F \cdot (1 - M) \cdot y_4^2 \cdot y_3 - 2 \cdot F \cdot (1 - M) \cdot \omega_T^2 \cdot y_3, \end{aligned} \quad (31a)$$

$$\begin{aligned}
F_2 = & -\frac{2 \cdot M}{(1-M)} \cdot y_1 \cdot y_2 \cdot y_4 \cdot y_5 + 4 \cdot y_2 \cdot y_3 \cdot y_4 \cdot y_7 + \\
& + 2 \cdot (I_1 L - F^2) \cdot y_1 \cdot y_4^2 - \frac{M}{(1-M)} \cdot y_1^3 \cdot y_4^2 - \frac{M}{(1-M)} \cdot y_1 \cdot y_2^2 \cdot y_4^2 + \\
& + 2 \cdot y_1 \cdot y_3^2 \cdot y_4^2 - 2 \cdot \omega_b^2 \cdot (1-M) \cdot (I_1 L - F^2) \cdot y_1 + \\
& + \frac{M \cdot \omega_b^2 \cdot (1-M)}{(1-M)} \cdot y_1^3 + \frac{\omega_b^2 \cdot M \cdot (1-M)}{(1-M)} \cdot y_1 \cdot y_2^2 - 2 \cdot \omega_b^2 \cdot (1-M) \cdot y_3^2 \cdot y_1 - \\
& - 4 \cdot (I_1 \cdot L - F^2) \cdot y_4 \cdot y_6 + \frac{2 \cdot M \cdot y_4^2}{(1-M)} \cdot y_4 \cdot y_6 - 4 \cdot y_4 \cdot y_6 \cdot y_3^2 - \\
& - 2 \cdot F \cdot (y_4^2 - \omega_T^2) \cdot y_2 \cdot y_3,
\end{aligned} \tag{31b}$$

$$\begin{aligned}
F_3 = & \frac{2 \cdot M}{(1-M)} \cdot y_1 \cdot y_2 \cdot y_4 \cdot y_6 - 4 \cdot y_1 \cdot y_3 \cdot y_4 \cdot y_7 - \\
& - 2 \cdot (I_1 \cdot L - F^2) \cdot \omega_b^2 \cdot (1-M) \cdot y_2 + \omega_b^2 \cdot M \cdot y_1^2 \cdot y_2 + \omega_b^2 \cdot M \cdot y_2^3 - \\
& - 2 \cdot \omega_b^2 \cdot (1-M) \cdot y_2 \cdot y_3^2 + 2 \cdot (I_1 \cdot L - F^2) \cdot y_2 \cdot y_4^2 - \\
& - \frac{M}{(1-M)} \cdot y_1^2 \cdot y_2 \cdot y_4^2 - \frac{M}{(1-M)} \cdot y_2^3 \cdot y_4^2 + 2 \cdot y_2 \cdot y_3^2 \cdot y_4^2 + \\
& + 4 \cdot (I_1 \cdot L - F^2) \cdot y_4 \cdot y_5 - \frac{2 \cdot M}{(1-M)} \cdot y_2^2 \cdot y_4 \cdot y_5 + 4 \cdot y_3^2 \cdot y_4 \cdot y_5 + \\
& + 2 \cdot F \cdot y_1 \cdot y_3 \cdot y_4^2 - 2 \cdot F \cdot \omega_T^2 \cdot y_1 \cdot y_3,
\end{aligned} \tag{31c}$$

$$\begin{aligned}
F_4 = & 2 \cdot F \cdot M \cdot y_1 \cdot y_4 \cdot y_5 + 2 \cdot F \cdot M \cdot y_2 \cdot y_4 \cdot y_6 - 4 \cdot F \cdot (1-M) \cdot y_3 \cdot y_4 \cdot y_7 + \\
& + 2 \cdot (1-M) \cdot I_1 \cdot L \cdot y_3 \cdot y_4^2 - M \cdot y_1^2 \cdot y_3 \cdot y_4^2 - M \cdot y_2^2 \cdot y_3 \cdot y_4^2 + \\
& + 2 \cdot (1-M) \cdot y_3^3 \cdot y_4^2 - 2 \cdot (1-M) \cdot I_1 \cdot L \cdot \omega_T^2 \cdot y_3 + M \cdot \omega_T^2 \cdot y_1^2 \cdot y_3 + \\
& + M \cdot \omega_T^2 \cdot y_2^2 \cdot y_3 - 2 \cdot (1-M) \cdot \omega_T^2 \cdot y_3^3.
\end{aligned} \tag{31d}$$

#### Equations defining the perpetual points

Before proceeding with linearization around the restricted system's fixed points, the system's (4), (6) perpetual points, by setting accelerations and jerks equal to zero, are determined. The equations of jerks by differentiation of equations (4) with respect to time can be obtained, and in an explicit form, they are given by,

$$\begin{aligned}
[\mathbf{M}_{tot}] \cdot \begin{Bmatrix} \ddot{\theta} \\ \ddot{q}_v \\ \ddot{q}_w \\ \ddot{q}_\phi \end{Bmatrix} + [\mathbf{M}_{tot}] \cdot \begin{Bmatrix} \ddot{\theta} \\ \ddot{q}_v \\ \ddot{q}_w \\ \ddot{q}_\phi \end{Bmatrix} = \begin{Bmatrix} \dot{h}_1 \\ \dot{h}_2 \\ \dot{h}_3 \\ \dot{h}_4 \end{Bmatrix} \Leftrightarrow \\
\Leftrightarrow \begin{Bmatrix} \ddot{\theta} \\ \ddot{q}_v \\ \ddot{q}_w \\ \ddot{q}_\phi \end{Bmatrix} = [\mathbf{M}_{tot}]^{-1} \cdot \begin{Bmatrix} \dot{h}_1 \\ \dot{h}_2 \\ \dot{h}_3 \\ \dot{h}_4 \end{Bmatrix} - [\mathbf{M}_{tot}] \cdot \begin{Bmatrix} \ddot{\theta} \\ \ddot{q}_v \\ \ddot{q}_w \\ \ddot{q}_\phi \end{Bmatrix}.
\end{aligned} \tag{32}$$

Considering that for the determination of the perpetual points the accelerations are equal to zero, then lead to,

$$\begin{pmatrix} \ddot{\theta} \\ \ddot{q}_v \\ \ddot{q}_w \\ \ddot{q}_\phi \end{pmatrix} = [M_{tot}]^{-1} \begin{pmatrix} \dot{h}_1 \\ \dot{h}_2 \\ \dot{h}_3 \\ \dot{h}_4 \end{pmatrix} = [M_{tot}]^{-1} \begin{pmatrix} -2 \cdot \dot{\theta} \cdot \dot{q}_v^2 - 2 \cdot \dot{\theta} \cdot \dot{q}_w^2 - 4 \cdot \dot{\theta} \cdot \dot{q}_\phi^2 \\ [\dot{\theta}^2 - \omega_b^2 \cdot (1 - M)] \cdot \dot{q}_v \\ [\dot{\theta}^2 - \omega_b^2 \cdot (1 - M)] \cdot \dot{q}_w \\ (\dot{\theta}^2 - \omega_T^2) \cdot \dot{q}_\phi \end{pmatrix}. \quad (33)$$

The perpetual points in [7], by setting the accelerations given by the equations (6), and the equations (33), equal to zero, are determined for non-zero velocities.

*Perpetual manifolds and the sets of fixed points of the restricted system*

The sets of PPs of the original system eq. (6) with the sets defining the equilibria of the restricted system of equations (30a-d) coincide. The following three sets of points define them:

1. The first set of perpetual points ( $y_{1,0}$ ), is given by,

$$\begin{aligned} y_{1,0} &= (y_{0,1}, y_{0,2}, y_{0,3}, y_{0,4}, y_{0,5}, y_{0,6}, y_{0,7}) = \\ &= (q_{0,v}, q_{0,w}, q_{0,\phi}, \dot{\theta}_0, \dot{q}_{0,v}, \dot{q}_{0,w}, \dot{q}_{0,\phi}) = (0,0,0, \dot{\theta}_0, 0,0,0), \text{with } \dot{\theta}_0 \in \mathbb{R}, \end{aligned} \quad (34a)$$

which is a set for arbitrary values of the rotating speed but all the rest deformations and velocities of the shaft are zero.

2. The second set of perpetual points ( $y_{2,0}$ ) is given by,

$$\begin{aligned} y_{2,0} &= (y_{0,1}, y_{0,2}, y_{0,3}, y_{0,4}, y_{0,5}, y_{0,6}, y_{0,7}) = \\ &= (q_{0,v}, q_{0,w}, q_{0,\phi}, \dot{\theta}_0, \dot{q}_{0,v}, \dot{q}_{0,w}, \dot{q}_{0,\phi}) = \\ &= (q_{0,v}, q_{0,w}, 0, \pm\omega_b \cdot \sqrt{(1 - M)}, 0,0,0), \text{with } (q_{0,v}, q_{0,w}) \in \mathbb{R}^2, \end{aligned} \quad (34b)$$

which is a family for a rotating speed correlated with the natural frequency of lateral bending deformation, and the shaft can have any arbitrary values for lateral bending deformation, but the torsional position and all the velocities are zero.

3. The third set of perpetual points ( $y_{3,0}$ ) is given by,

$$\begin{aligned} y_{3,0} &= (y_{0,1}, y_{0,2}, y_{0,3}, y_{0,4}, y_{0,5}, y_{0,6}, y_{0,7}) = \\ &= (q_{0,v}, q_{0,w}, q_{0,\phi}, \dot{\theta}_0, \dot{q}_{0,v}, \dot{q}_{0,w}, \dot{q}_{0,\phi}) = \\ &= (0,0, q_{0,\phi}, \pm\omega_T, 0,0,0), \text{with } q_{0,\phi} \in \mathbb{R}, \end{aligned} \quad (34c)$$

a set accepting arbitrary values for torsional deformation of the shaft, a specific value of rotating speed relative to the torsional frequency, but the lateral bending deformation and all the velocities are zero.

The PPs of the original system eqs. (4), (6) or otherwise stated the equilibria of the restricted system of equations (30a-d) are not just a few points, but they are infinite points, and they form manifolds that in case of equilibria they are called equilibrium manifolds as explained in [14]. Similarly, the sets of PPs with infinite points are called Perpetual Manifolds (PMs).

The considered restricted system is fully decoupled by the equation describing the rigid body angular position's motion. So a fixed point in the restricted system

considering the constant value of the rigid body angular velocity as defined by the equilibria,

$$y_{0,4} = x_5 = \dot{\theta}_0 = ct, \quad (35a)$$

and then through the first equation of the system of equations (9) the angular position  $\theta \in S^1$  is given by,

$$x_1 = \theta = \dot{\theta}_0 \cdot t + \theta_0, \quad (35b)$$

which are periodic rigid body motions of the spinning shaft with period,

$$T = \frac{2\pi}{\dot{\theta}_0}. \quad (35c)$$

Therefore, these solutions form families of normal modes with the rigid body motions of the spinning shaft. More precisely,

- The first set of the PPs/equilibria given by equation (34a) defines dynamics that the shaft is spinning with any constant angular velocity ( $\dot{\theta}_0 \in \mathbb{R}$ ) in rigid body rotation without any deformation and forms the 1<sup>st</sup> PM.

- The second set of the PPs/equilibria given by equation (34b) defines dynamics that the shaft is spinning with a specific constant value of angular velocity ( $\dot{\theta}_0 = \pm\omega_b \cdot \sqrt{(1-M)}$ ) in rigid body rotation with any lateral bending constant deformation ( $(q_{0,v}, q_{0,w}) \in \mathbb{R}^2$ ), but with zero torsional deformation, and forms the 2<sup>nd</sup> PM.

- The third set of the PPs/equilibria given by equation (34c) defines dynamics that the shaft is spinning with a specific constant value of angular velocity ( $\dot{\theta}_0 = \pm\omega_T$ ) in rigid body rotation with any constant torsional deformation ( $q_{0,\phi} \in \mathbb{R}$ ) value, but with zero lateral bending deformation, and forms the 3<sup>rd</sup> PM.

### Linearization around the perpetual points/fixed points of the restricted system

Therefore, in the previous subsection, the two ways to determine the rigid body modes/motions of the spinning shaft are shown. The linearization equations around the three sets of points/PMs, given by eq. (32), using equations (30) or equations (9) are the same with the only difference that in the latter, there is the existence of one more decoupled equation that defines the rigid body angular position.

The linearization is performed to the restricted system using the following perturbations ( $(\xi_i, i = 1, \dots, 7)$ ) [3],

$$\begin{aligned} y &= (y_1, y_2, y_3, y_4, y_5, y_6, y_7) = (q_v, q_w, q_\phi, \theta, \dot{q}_v, \dot{q}_w, \dot{q}_\phi) = \\ &= (y_{0,1} + \xi_1, y_{0,2} + \xi_2, y_{0,3} + \xi_3, y_{0,4} + \xi_4, y_{0,5} + \xi_5, y_{0,6} + \xi_6, y_{0,7} + \xi_7), \end{aligned} \quad (36)$$

lead to,

$$\{\dot{\xi}_1 \ \dot{\xi}_2 \ \dot{\xi}_3 \ \dot{\xi}_4 \ \dot{\xi}_5 \ \dot{\xi}_6 \ \dot{\xi}_7\}^T = [J_y]_{y_0^{(i)}} \cdot \{\xi_1 \ \xi_2 \ \xi_3 \ \xi_4 \ \xi_5 \ \xi_6 \ \xi_7\}^T, \quad (37)$$

with  $i=1,2,3$ ,

and the Jacobian ( $J_y$ ) can be split into upper ( $J_{y,u}$ ) and lower ( $J_{y,l}$ ) parts as follows,

$$[J_y] = \begin{bmatrix} J_{y,u} \\ J_{y,l} \end{bmatrix}. \quad (38)$$

The upper part of the Jacobian matrix  $-\mathbf{[J_{y,u}]}$  is given by,

$$\mathbf{[J_{y,u}]} = \begin{bmatrix} 0 & 0 & 0 & 0 & 1 & 0 & 0 \\ 0 & 0 & 0 & 0 & 0 & 1 & 0 \\ 0 & 0 & 0 & 0 & 0 & 0 & 1 \end{bmatrix} = ct, \quad (39)$$

and the lower part of the Jacobian matrix  $-\mathbf{[J_{y,l}]}$  is given by,

$$\mathbf{[J_{y,l}]} = \left[ -\frac{1}{\delta^2} \cdot \frac{\partial \delta}{\partial y_j} \cdot F_i + \frac{1}{\delta} \cdot \frac{\partial F_i}{\partial y_j} \right], \quad (40)$$

it should be noted,

$$F_i = 0. \quad (41)$$

Therefore, the lower part of the Jacobian  $-\mathbf{[J_{y,l}]}$  is given by,

$$\mathbf{[J_{y,l}]}|_{y_0} = \left[ \frac{1}{\delta} \cdot \frac{\partial F_i}{\partial y_j} \right]_{y_0}. \quad (42)$$

with regards to the Hessian since the upper part of the Jacobian is constant ( $\mathbf{[J_{y,u}]} = ct$ ) the determinant of the Hessian is zero, therefore; *all the equilibria of the restricted system are degenerate.*

*Linearization around the 1<sup>st</sup> perpetual manifold*

Linearization around the 1<sup>st</sup> PM of the restricted system, with the perturbations denoted by adding the **1** as first bold-index ( $(\xi_{1,i}, \text{for } i = 1, \dots, 7)$ ) resulting in the following sets of differential equations [3]:

The linearized equations that describe the motion are given by,

$$\dot{\xi}_{1,3} = \xi_{1,7}, \quad (43a)$$

$$\dot{\xi}_{1,4} = F \cdot a_2 \cdot \xi_{1,3}, \quad (43b)$$

$$\dot{\xi}_{1,7} = I_1 \cdot L \cdot a_2 \cdot \xi_{1,3}. \quad (43c)$$

that lead to,

$$\ddot{\xi}_{1,3} - I_1 \cdot L \cdot a_2 \cdot \xi_{1,3} = 0, \quad (44)$$

and the lateral bending motions are described by,

$$\begin{Bmatrix} \dot{\xi}_{1,1} \\ \dot{\xi}_{1,2} \\ \dot{\xi}_{1,5} \\ \dot{\xi}_{1,6} \end{Bmatrix} = \begin{bmatrix} 0 & 0 & 1 & 0 \\ 0 & 0 & 0 & 1 \\ a_1 & 0 & 0 & -a_3 \\ 0 & a_1 & a_3 & 0 \end{bmatrix} \cdot \begin{Bmatrix} \xi_{1,1} \\ \xi_{1,2} \\ \xi_{1,5} \\ \xi_{1,6} \end{Bmatrix}, \quad (45)$$

whereas,

$$\delta(y_0^{(1)}) = 2 \cdot (1 - M) \cdot (I_1 \cdot L - F^2), \quad (46a)$$

$$a_1(\dot{\theta}_0) = \frac{(\dot{\theta}_0^2 - \omega_b^2 \cdot (1 - M))}{(1 - M)}, \quad (46b)$$

$$a_2(\dot{\theta}_0) = \frac{(\dot{\theta}_0^2 - \omega_T^2)}{(I_1 \cdot L - F^2)}, \quad (46c)$$

$$a_3(\dot{\theta}_0) = \frac{2 \cdot \dot{\theta}_0}{(1 - M)}. \quad (46d)$$

The dynamics, by the same systems of differential equations obtained with the 1<sup>st</sup> order approximation of the multiple scales analysis of the previous section [3], is described. More precisely, the differential equation (44) of the linearized system that describes the perturbed torsional modal displacement ( $q_\phi$ ), then with the exchange of the notation of the variable  $\xi_{1,3}$  with  $q_\phi$ , and considering equation (46c) in equation (44) leads to the equation (17a) that describes the same motion in 1<sup>st</sup> order approximation in multiple scales analysis.

Similarly, the system of equations (22a-b) that describes the lateral bending motions in 1<sup>st</sup> order approximation of multiple-scale analysis is the same as the system eq. (45) describing the perturbed lateral bending modal displacements of the linearized equations with the 1<sup>st</sup> set of equilibrium points. Considering the equation (45), this can become profound by exchanging the perturbation velocities  $\dot{\xi}_{1,5}$ , with  $\dot{q}_v$ ,  $\dot{\xi}_{1,6}$  with  $\dot{q}_w$ , and the perturbations  $\xi_{1,1}$ , with  $q_v$  and  $\xi_{1,3}$  with  $q_w$  respectively, by also taking into account the explicit definitions of constants that are given by the equations (46b,d).

*Linearization around the 2<sup>nd</sup> perpetual manifold*

Linearization around the 2<sup>nd</sup> PM of the restricted system, with the perturbations denoted by adding the **2** as the first index ( $\xi_{2,i}$ , for  $i = 1, \dots, 7$ ) resulting in the following sets of differential equations [3]:

The system of differential equations is given by,

$$\dot{\xi}_{2,3} = \xi_{2,7}, \quad (47a)$$

$$\dot{\xi}_{2,4} = c_9 \cdot \xi_{2,3} + c_1 \cdot \xi_{2,5} + c_2 \cdot \xi_{2,6}, \quad (47b)$$

$$\dot{\xi}_{2,5} = -c_8 \cdot y_{0,2} \cdot \xi_{2,3} + c_3 \cdot y_{0,1} \cdot \xi_{2,4} - c_7 \cdot \xi_{2,5} - c_4 \cdot \xi_{2,6}, \quad (47c)$$

$$\dot{\xi}_{2,6} = c_8 \cdot y_{0,1} \cdot \xi_{2,3} + c_3 \cdot y_{0,2} \cdot \xi_{2,4} + c_5 \cdot \xi_{2,5} + c_7 \cdot \xi_{2,6}, \quad (47d)$$

$$\dot{\xi}_{2,7} = c_6 \cdot \xi_{2,3} + F \cdot c_1 \cdot \xi_{2,5} + F \cdot c_2 \cdot \xi_{2,6}, \quad (47e)$$

and then, the other perturbed variables arise with direct integration of,

$$\dot{\xi}_{2,1} = \xi_{2,5}, \quad (47f)$$

$$\dot{\xi}_{2,2} = \xi_{2,6}. \quad (47g)$$

whereas,

$$c_1(y_{0,1}, y_{0,2}) = \frac{2 \cdot M \cdot y_{0,1} \cdot \omega_b \cdot \sqrt{(1-M)}}{\delta(y_0^{(2)})}, \quad (48a)$$

$$c_2(y_{0,1}, y_{0,2}) = \frac{2 \cdot M \cdot y_{0,2} \cdot \omega_b \cdot \sqrt{(1-M)}}{\delta(y_0^{(2)})}, \quad (48b)$$

$$c_3 = \frac{2 \cdot \omega_b \cdot \sqrt{(1-M)}}{(1-M)}, \quad (48c)$$

$$c_4(y_{0,1}, y_{0,2}) = \frac{2 \cdot \omega_b \cdot \sqrt{(1-M)} \cdot [2 \cdot (1-M) \cdot (I_1 \cdot L - F^2) - M \cdot y_{0,1}^2]}{(1-M) \cdot \delta(y_0^{(2)})}, \quad (48d)$$

$$c_5(y_{0,1}, y_{0,2}) = \frac{2 \cdot \omega_b \cdot \sqrt{(1-M)} \cdot [2 \cdot (1-M) \cdot (I_1 \cdot L - F^2) - M \cdot y_{0,2}^2]}{(1-M) \cdot \delta(y_0^{(2)})}, \quad (48e)$$

$$c_6(y_{0,1}, y_{0,2}) = \frac{(2 \cdot (1-M) \cdot I_1 \cdot L - M \cdot y_{0,1}^2 - M \cdot y_{0,2}^2)(\omega_b^2 \cdot (1-M) - \omega_T^2)}{\delta(y_0^{(2)})}, \quad (48f)$$

$$c_7(y_{0,1}, y_{0,2}) = \frac{2 \cdot M \cdot y_{0,1} \cdot y_{0,2} \cdot \omega_b \cdot \sqrt{(1-M)}}{(1-M) \cdot \delta(y_0^{(2)})}, \quad (48g)$$

$$c_8(y_{0,1}, y_{0,2}) = \frac{2 \cdot F \cdot (\omega_b^2 \cdot (1-M) - \omega_T^2)}{\delta(y_0^{(2)})}, \quad (48h)$$

$$c_9(y_{0,1}, y_{0,2}) = \frac{2 \cdot F \cdot (1-M) \cdot (\omega_b^2 \cdot (1-M) - \omega_T^2)}{\delta(y_0^{(2)})}, \quad (48i)$$

and,

$$\delta(y_0^{(2)}) = 2 \cdot (1-M) \cdot (I_1 \cdot L - F^2) - M \cdot y_{0,1}^2 - M \cdot y_{0,2}^2, \quad (48j)$$

$$f_1 = \omega_T^2 - \omega_b^2 \cdot (1-M). \quad (48k)$$

The eigenvalues of the Jacobian are given by,

$$\eta_{1 \div 3} = 0, \quad (49a-c)$$

$$\eta_{4 \div 7}(z) = \pm i \cdot \sqrt{\frac{p_0 + p_1 \cdot z \mp \sqrt{(r_1 \cdot z - r_2)^2 + r_3^2 \cdot z}}{2 \cdot \delta}} = \pm i \cdot H_{1 \div 2}. \quad (49d-g)$$

whereas,

$$z = y_{0,1}^2 + y_{0,2}^2, \quad (50a)$$

$$p_0 = 8 \cdot \omega_b^2 \cdot (I_1 \cdot L - F^2) + 2 \cdot (1-M) \cdot I_1 \cdot L \cdot f_1, \quad (50b)$$

$$p_1 = -M \cdot (4 \cdot \omega_b^2 + f_1), \quad (50c)$$

$$r_1 = M \cdot (4 \cdot \omega_b^2 - f_1), \quad (50d)$$

$$r_2 = 2 \cdot [4 \cdot \omega_b^2 \cdot (I_1 \cdot L - F^2) - (1-M) \cdot I_1 \cdot L \cdot f_1], \quad (50e)$$

$$r_3^2 = 32 \cdot M^2 \cdot \omega_b^2 \cdot f_1 \cdot F^2. \quad (50f)$$

*Linearization around the 3<sup>rd</sup> perpetual manifold*

Linearization around the 3<sup>rd</sup> PM of the restricted system lead to, with the perturbations denoted by adding the 3 as first index ( $\xi_{3,i}$ , for  $i = 1, \dots, 7$ ) resulting in the following sets of differential equations [3]:

The systems of differential equations are given by,

- First system

$$\dot{\xi}_{3,3} = \xi_{3,7}, \quad (51)$$

- Second system

$$\dot{\xi}_{3,4} = b_1 \cdot F \cdot \xi_{3,4} - b_1 \cdot \xi_{3,7}, \quad (52a)$$

$$\dot{\xi}_{3,7} = b_1 \cdot b_3 \cdot \xi_{3,4} - F \cdot b_1 \cdot \xi_{3,7}, \quad (52b)$$

which describes coupled motions of rigid body angular velocity with torsional 'modal' displacement.

- Third system

$$\dot{\xi}_{3,1} = \xi_{3,5}, \quad (53a)$$

$$\dot{\xi}_{3,2} = \xi_{3,6}, \quad (53b)$$

$$\dot{\xi}_{3,5} = b_2 \cdot f_1 \cdot \xi_{3,1} - 2 \cdot b_2 \cdot \omega_T \cdot \xi_{3,6}, \quad (53c)$$

$$\dot{\xi}_{3,6} = b_2 \cdot f_1 \cdot \xi_{3,2} + 2 \cdot b_2 \cdot \omega_T \cdot \xi_{3,5}. \quad (53d)$$

which describes the lateral bending motions. The parameters are given by,

$$b_1(y_{0,3}) = \frac{2 \cdot \omega_T \cdot y_{0,3}}{(I_1 \cdot L - F^2 + y_{0,3}^2)}, \quad (54a)$$

$$b_2 = \frac{1}{(1-M)}, \quad (54b)$$

$$b_3(y_{0,3}) = I_1 \cdot L + y_{0,3}^2. \quad (54c)$$

The eigenvalues are given by,

$$\mu_1 = 0, \quad (55a)$$

$$\mu_{2,3}(y_{0,3}) = \pm b_1 \cdot \sqrt{(F^2 - b_3)} = \pm i \cdot \frac{2 \cdot \omega_T \cdot y_{0,3}}{\sqrt{(I_1 \cdot L - F^2 + y_{0,3}^2)}} = \pm i \cdot M_1, \quad (55b)$$

$$\begin{aligned} \mu_{4 \div 7} &= \pm \frac{i}{(1-M)} \\ &\cdot \sqrt{(1+M) \cdot \omega_T^2 + (1-M)^2 \cdot \omega_b^2 \mp 2 \cdot \omega_T \cdot \sqrt{M \cdot \omega_T^2 + \omega_b^2} \cdot (1-M)^2} = \\ &= \pm i \cdot M_{3 \div 4} = ct. \end{aligned} \quad (55c)$$

The explicit solution of the second system eq. (52a,b) is given by [3],

$$\xi_{3,4} = (A_R + i \cdot A_I) \cdot e^{i \cdot M_1 \cdot t} + cc, \quad (56a)$$

$$\xi_{3,7} = (B_R + i \cdot B_I) \cdot e^{i \cdot M_1 \cdot t} + cc, \quad (56b)$$

with,

$$A_R = \frac{\xi_{3,4}(0)}{2}, \quad (56c)$$

$$A_I = \frac{(\xi_{3,7}(0) - F \cdot \xi_{3,4}(0))}{2 \cdot \sqrt{b_3 - F^2}}, \quad (56d)$$

and

$$B_R = \frac{\xi_{3,7}(0)}{2}, \quad (56e)$$

$$B_I = \frac{(F \cdot \xi_{3,7}(0) - b_3 \cdot \xi_{3,4}(0))}{2 \cdot \sqrt{b_3 - F^2}}. \quad (56f)$$

The last perturbed variable ( $\xi_3$ ) is given through direct integration of equation (122b) and it is given by,

$$\xi_{3,3} = \frac{\xi_{3,3}(0)}{2} - \frac{B_I}{M_1} - \frac{i \cdot (B_R + i \cdot B_I)}{M_1} e^{i \cdot M_1 \cdot t} + cc. \quad (56g)$$

The final solution is given by,

$$y = (y_1, y_2, y_3, y_4, y_5, y_6, y_7) = (0, 0, y_{0,3,cr} + \xi_{3,3}, \omega_T + \xi_{3,4}, 0, 0, \xi_{3,7}). \quad (57)$$

This system can also be considered as a perturbed linearized system of the 1<sup>st</sup> family of fixed points at rotating velocity ( $\dot{\theta}_0 = \omega_T$ ) with  $y_3 = \xi_{1,3} = y_{0,3,cr}$ , therefore

it is expected that positive perturbation of the angular velocity ( $\xi_{3,4}(0) > 0$ ) leads to a non-periodic solution of the original system, but negative perturbations can lead to periodic orbits.

In the 3<sup>rd</sup> PM, all the eigenvalues of the Jacobian are purely imaginary. The eigenvalues associated with lateral bending motions are constant on the 3<sup>rd</sup> PM, therefore with the same eigenvalues of the 1<sup>st</sup> PM on this rotating speed, and the motion is described by the equations (A.20a-d).

**Backbone lines of the rigid body modes with the eigenvalues of the linearized systems around them.**

As in the previous section is shown, the equilibrium manifolds of the restricted system are the same as the perpetual manifolds of the original system, and they are given by the equations (32a-c). They are three PMs and define the rigid body modes of the shaft spinning with non-constant rotating speed. The physical deformation of the shaft in the lateral bending motion, by the radial deformation is defined by combining the two lateral bending modal deformations ( $y_{01}, y_{02}$ ). Therefore the two lateral bending deformation modal displacements can be considered together without losing any information, and considering all the rest generalized coordinates that form the PMs, a 3D plot, that is, the projection of the PMs, can be drawn. In Figure 2, the projected to 3D PMs are plotted, and they form the backbone lines of the rigid body modes. In Figure-2, the 1<sup>st</sup>-PM is formed by the line with any value of rigid body angular velocity and all the generalized rest coordinates being zero.

The 2<sup>nd</sup>-PM is the line with angular velocity  $\omega_b \cdot \sqrt{1-M}$ , with any value of lateral bending modal displacements for zero torsional ‘modal’ displacement. The 3<sup>rd</sup>-PM is the line with angular velocity  $-\omega_T$ , with any value of torsional ‘modal’ displacement, and with zero modal displacements for lateral bending motion.

Moreover, in Figure 2, the associated eigenvalues, obtained from the dynamical systems arisen by the linearization of the original dynamical system to the three PMs, are shown. The  $\lambda_i$  – eigenvalues indicated near the line of the first set of perpetual manifolds, obtained from the linearization around the 1<sup>st</sup> PM, and are the same that describe the motion in the 1<sup>st</sup> order approximation of the multiple scale analysis. The  $\eta_i$  – eigenvalues indicated near the vertical line correspond to the linearization around the 2<sup>nd</sup> set of perpetual manifolds. The  $\mu_i$  – eigenvalues indicated near the 3<sup>rd</sup> PM line correspond to the linearization around the 3<sup>rd</sup> perpetual manifold.

In Figure 2, two regions can be identified based on the eigenvalue’s qualitative characteristics. One region is defined by the cyan line for rigid body angular velocity,

$$\dot{\theta}_0 = \frac{\omega_b(1-M)}{\sqrt{-M}}, \quad (58)$$

that the 1<sup>st</sup> PM describes the motion. The eigenvalues that are associated with the lateral bending motion as long as the angular velocity is less than the given by equation (58) value, that the trajectory is on the ‘Line (side-),’ are purely imaginary  $\lambda_{4\pm 7}(y_{0,4}) = \pm i \cdot \omega_{1,2}$ . As long as the trajectory is crossing the cyan line and move to the ‘Line (side+),’ the eigenvalues associated with lateral bending dynamics are not pure imaginary any longer ( $\lambda_{4\pm 7} = \pm(A_6 \pm i \cdot A_7)$ ).

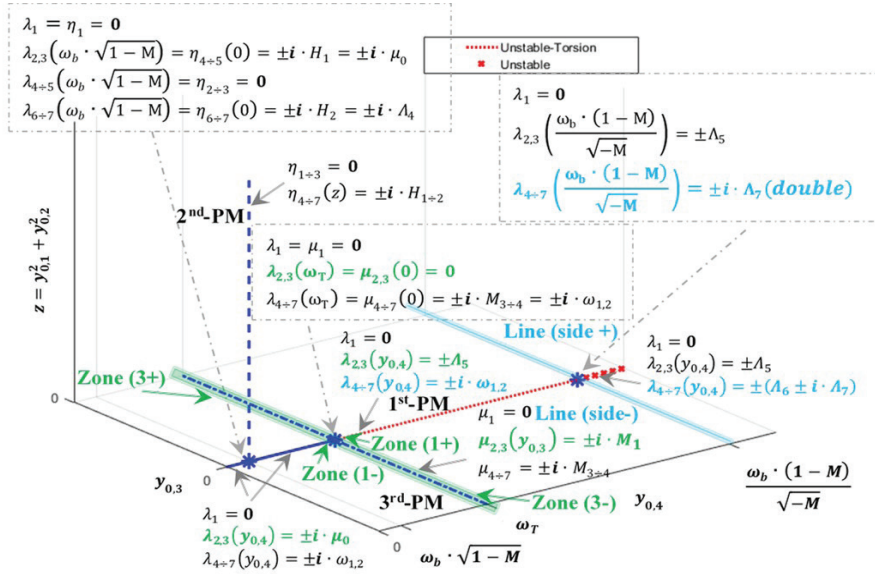


FIGURE 2. Perpetual manifolds (PMs)/backbone curves of the rigid body normal modes overall manifold projected to 3D, with the associated eigenvalues of the linearized system around them, indicating the stability regions, and incorporating the two regions ('Green zone', and 'Cyan line') that the eigenvalues are changing qualitatively with respect to the angular velocity.

The second region is the green 'Zone,' centred in the angular velocity  $\dot{\theta}_0 = \omega_T$ . There is a qualitative change of the eigenvalues of the dynamical system describing the dynamics in torsion from pure imaginary to real.

The system's eigenvalues describing the torsional/rigid body angular velocity dynamics near this region are with bold green fonts. For almost zero values of torsional 'modal' displacement, the motion is described by the linearization around the 1<sup>st</sup>-PM. For smaller values of the angular velocity than  $\omega_T$  that the system is in 'Zone (1-)' the eigenvalues are pure complex ( $\lambda_{2,3} = \pm i \cdot \mu_0$ ). Whereas the trajectory is crossing the threshold for angular velocity equal to  $\omega_T$  they become zero and then for greater values of angular velocity that the trajectory is in 'Zone (1+)' they become real ( $\lambda_{2,3} = \pm \Lambda_5$ ). Also, as long as the part of the trajectory corresponds to high values of torsional 'modal' displacement, and with angular velocity close to  $\omega_T$ , then the trajectory is in green 'Zones ( $\pm 3$ )', and the dynamics is described by the 3<sup>rd</sup> set of PM, with eigenvalues ( $\mu_{2,3} = \pm i \cdot M_1$ ). Therefore there is a qualitative difference in the solutions of the trajectory, for the torsional and rigid body angular velocity dynamics, at different parts of the green 'Zone'.

The positive real eigenvalues in the differential equations solution are called Lyapunov exponents, and they are associated with chaotic motion. A trajectory that crosses all the regions of the green 'zone' in fig. 2 with different qualitative

eigenvalues means the motion is chaotic with variant Lyapunov exponents. The torsional/rigid body angular velocity dynamic analysis in [4] has been done based on this observation. More precisely, the different solutions of the torsional motion on green region considered and the trajectory they form on each zone of this region is determined as follows.

The systems of differential equations that describe the motions around the 1<sup>st</sup> and 3<sup>rd</sup> PM are used for the projection to the phase space by parameterizing time with respect to the perturbation in torsional position ( $\xi_{1,3}$ , and  $\xi_{3,3}$ , respectively).

Using the linearized equations (43b-c) and (44) with  $\xi_{1,i}$  perturbations around the 1<sup>st</sup> PM, and parameterization of time leads to [4],

$$\frac{d\xi_{1,4}}{d\xi_{1,3}} = \frac{F \cdot (\dot{\theta}_0^2 - \omega_T^2) \cdot \xi_{1,3}}{(I_1 \cdot L - F^2) \cdot \xi_{1,7}}, \tag{59}$$

$$\frac{d\xi_{1,7}}{d\xi_{1,3}} = \frac{I_1 \cdot L \cdot (\dot{\theta}_0^2 - \omega_T^2) \cdot \xi_{1,3}}{(I_1 \cdot L - F^2) \cdot \xi_{1,7}} \Leftrightarrow \xi_{1,7}^2 - \frac{I_1 \cdot L \cdot (\dot{\theta}_0^2 - \omega_T^2)}{(I_1 \cdot L - F^2)} \cdot \xi_{1,3}^2 = A \Leftrightarrow$$

$$\Leftrightarrow \dot{q}_\phi^2 - \frac{I_1 \cdot L \cdot (\dot{\theta}_0^2 - \omega_T^2)}{(I_1 \cdot L - F^2)} \cdot q_\phi^2 = A, \tag{60a-c}$$

whereas,  $\xi_{1,7} \neq 0$ . The zero value corresponds to the local extrema of perturbation of torsional position ( $\xi_{1,3}$ ), and they can be neglected without changing the qualitative characteristics of the analysis. Angular velocity greater than  $\omega_T$  corresponds to a family of hyperbolas with center (0,0) in phase space, and they approximate well the orbit near the region defined by the green ‘Zone (1+)’ of fig. 2 which corresponds to almost zero torsional modal displacements. Whenever the angular velocity is equal to  $\omega_T$  lead to a constant perturbation in torsional velocity ( $\xi_{1,7}$ ) and finally for angular velocity less than  $\omega_T$  the orbit are crossing the region of green ‘Zone (1-)’ of fig. 2 with almost zero torsional modal displacements. A family of ellipses with center (0,0) in phase space, is describing this part of the orbit. Using equation (60b), the constant of integration A can be determined. Rearrangement of equation (60c) lead to [4],

$$\xi_{1,7} = \pm \sqrt{\frac{I_1 \cdot L \cdot (\dot{\theta}_0^2 - \omega_T^2)}{(I_1 \cdot L - F^2)} \cdot \xi_{1,3}^2 + A} \Leftrightarrow \dot{q}_\phi = \pm \sqrt{\frac{I_1 \cdot L \cdot (\dot{\theta}_0^2 - \omega_T^2)}{(I_1 \cdot L - F^2)} \cdot q_\phi^2 + A}, \tag{61}$$

then using equation (61) in equation (59), and integrating while considering the original system state space variables lead to [4],

$$\dot{\theta} = \dot{\theta}_0 \pm \frac{F}{I_1 \cdot L} \cdot \sqrt{\frac{I_1 \cdot L \cdot (\dot{\theta}_0^2 - \omega_T^2)}{(I_1 \cdot L - F^2)} \cdot q_\phi^2 + A} + B, \tag{62}$$

with B being the integration constant, and they correspond to the following families of orbits [4],

$$\frac{(I_1 \cdot L)^2 \cdot (\dot{\theta} - \dot{\theta}_0 - B)^2}{F^2 \cdot A} - \frac{I_1 \cdot L \cdot (\dot{\theta}_0^2 - \omega_T^2)}{A \cdot (I_1 \cdot L - F^2)} \cdot q_\phi^2 = 1, \tag{63}$$

whereas for angular velocity greater than  $\omega_T$  corresponds to a family of hyperbolas with centre  $(\dot{\theta}_0 + B, 0)$ . Initial angular velocity ( $\dot{\theta}_0$ ) equal to  $\omega_T$  leads to a solution with constant rigid body angular velocity ( $\dot{\theta}$ ). Finally for angular velocity smaller than  $\omega_T$  lead to a family of ellipses with center  $(\dot{\theta}_0 + B, 0)$  in phase space.

The linearized namely 3<sup>rd</sup> PM with angular velocity equal to  $\omega_T$  is surrounded by periodic orbits. The constant perturbations in torsional and rigid body angular

velocities obtained from equations (62) and (63) respectively are not describing the orbits in this region. In this region near the green ‘Zones ( $\pm 3$ )’ of fig.2, with different than zero torsional modal displacements ( $|y_3| = |q_\phi| > 0$ ), a better approximation of the orbits by the linearization around the 3<sup>rd</sup> EM can be obtained. The orbits associated with the linearization around the 3<sup>rd</sup> EM with  $\xi_{3,i}$  – perturbations, by parametrizing time with the perturbation in torsional position ( $\xi_{3,3}$ ) using the equations (52a,b), are determined. Firstly, the differential equation [4],

$$\frac{d\xi_{3,4}}{d\xi_{3,7}} = \frac{F \cdot \xi_{3,4} - \xi_{3,7}}{(I_1 \cdot L + y_{0,3}^2) \cdot \xi_{3,4} - F \cdot \xi_{3,7}} \quad (64)$$

whereas the points corresponding to local extrema of the torsional velocity ( $\xi_{3,7}$ ) are neglected (without changing qualitative the conclusions of this analysis) with  $(I_1 \cdot L + y_{0,3}^2) \cdot \xi_{3,4} \neq F \cdot \xi_{3,7}$ . Solving equation (64) lead to [4],

$$\xi_{3,4} = \frac{F \cdot \xi_{3,7}}{(I_1 \cdot L + y_{0,3}^2)} \pm \frac{\sqrt{-(I_1 \cdot L - F^2 + y_{0,3}^2) \cdot \xi_{3,7}^2 + C}}{(I_1 \cdot L + y_{0,3}^2)} \quad (65)$$

Using any pair of values, the constant of integration C can be determined by the following rearranged equation [4],

$$(I_1 \cdot L + y_{0,3}^2)^2 \cdot \xi_{3,4}^2 + (I_1 \cdot L + y_{0,3}^2) \cdot \xi_{3,7}^2 - 2 \cdot (I_1 \cdot L + y_{0,3}^2) \cdot F \cdot \xi_{3,4} \cdot \xi_{3,7} - C = 0, \quad (66)$$

which is forming an ellipse.

The 2<sup>nd</sup> equation, for  $\xi_{3,7} \neq 0$ , is given by [4],

$$\frac{d\xi_{3,7}}{d\xi_{3,3}} = 2 \cdot \omega_T \cdot y_{0,3} \cdot \left( \frac{(I_1 \cdot L + y_{0,3}^2)}{(I_1 \cdot L - F^2 + y_{0,3}^2)} \cdot \frac{\xi_{3,4}}{\xi_{3,7}} - \frac{F}{(I_1 \cdot L - F^2 + y_{0,3}^2)} \right), \quad (67)$$

using (eq. 65) and direct integration lead to [4],

$$\xi_{3,3} = \mp \frac{1}{2 \cdot \omega_T \cdot y_{0,3}} \cdot \sqrt{-(I_1 \cdot L - F^2 + y_{0,3}^2) \cdot \xi_{3,7}^2 + C + D}, \quad (68)$$

or using state space variables of the original system and with rearrangement lead to the following family phase space curves [4],

$$[2 \cdot \omega_T \cdot y_{0,3} \cdot (q_\phi - y_{0,3} - D)]^2 + (I_1 \cdot L - F^2 + y_{0,3}^2) \cdot \xi_{3,7}^2 = C, \quad (69)$$

which are ellipsis centered at  $(y_3, y_7) = (y_{0,3} + D, 0)$  [3].

Rearrangement of equation (69) for a solution of perturbation of ‘modal’ torsional velocity with respect to perturbation of ‘modal’ torsional position lead to [4],

$$\xi_{3,7} = \pm \sqrt{\frac{C - [2 \cdot \omega_T \cdot y_{0,3} \cdot (\xi_{3,3} - D)]^2}{(I_1 \cdot L - F^2 + y_{0,3}^2)}} \Leftrightarrow y_7 = \pm \sqrt{\frac{C - [2 \cdot \omega_T \cdot y_{0,3} \cdot (q_\phi - y_{0,3} - D)]^2}{(I_1 \cdot L - F^2 + y_{0,3}^2)}}, \quad (70a)$$

and replacing eq. (70a) in eq. (65) using state space variables of the original system lead to [4],

$$\dot{\theta} = \omega_T \pm \frac{F}{(I_1 \cdot L + y_{0,3}^2)} \cdot \sqrt{\frac{C - [2 \cdot \omega_T \cdot y_{0,3} \cdot (q_\phi - y_{0,3} - D)]^2}{(I_1 \cdot L - F^2 + y_{0,3}^2)}} \pm \frac{2 \cdot \omega_T \cdot y_{0,3} \cdot (q_\phi - y_{0,3} - D)}{(I_1 \cdot L + y_{0,3}^2)}, \quad (70b)$$

and written as a 2<sup>nd</sup> order, that forms a family of ellipsis with center at  $(q_\phi, \dot{\theta}) = (y_{0,3} + D, \omega_T)$  can be easily concluded.

The curves in phase space, associated with each solution eq. (61), (69), (70b), with real and imaginary eigenvalues, in each zone, in [4] with the numerical solutions are compared. The analytical solutions approximate the trajectories, within the region of their validity, and they were in good agreement. The analytical verification of the variant Lyapunov exponents with numerical simulations in [4] is done, but further work for a thorough examination of chaotic motions of the spinning shaft e.g. domain of attraction of chaos etc, is needed.

**Normal modes from linearization around the perpetual manifolds.** In [3], based on the linearization around the perpetual manifolds, the associated normal modes are determined, and they are given by,

*Normal modes, around the 1<sup>st</sup> perpetual manifold*

They are associated with:

1) Perturbations in torsional motion have periodic solutions for the following critical speed [3],

$$\dot{\theta}_{0,T,cr,1,2} = \pm \sqrt{\frac{1}{2 \cdot (1 - \frac{4}{\pi^2})}} \cdot \omega_T = \pm 0.9169 \omega_T. \tag{71}$$

2) Perturbations in lateral bending motions, corresponding to the following rigid body angular velocities [3],

$$\dot{\theta}_{0,B,cr,1} = \omega_b \cdot (1 - M) \cdot \sqrt{\frac{M^2 - 5 \cdot M + 4}{M^4 - 6 \cdot M^3 + 9 \cdot M^2 - 4 \cdot M}} \tag{72a}$$

and

$$\dot{\theta}_{0,B,cr,2} = \omega_b \cdot (1 - M) \cdot \sqrt{\frac{M^2 - M}{M^4 - 6 \cdot M^3 + 9 \cdot M^2 - 4 \cdot M}} \tag{72b}$$

that must be perturbed for periodic lateral bending motions.

*Normal modes around the 3<sup>rd</sup> perpetual manifold*

They are associated with torsional motions and correspond to the following torsional ‘modal’ value [3],

$$q_{\phi,cr} = y_{0,3,cr} = \sqrt{\frac{I_1 \cdot L - F^2}{3}}, \tag{73}$$

which defines the equilibrium point that must be perturbed to find torsional periodic motions. This normal mode cannot directly obtained from the multiple scales analysis since, the associated equations of motion are not explicitly correlated with the 1<sup>st</sup> order approximation with the multiple scale analysis.

In the next section, the analytical findings with numerical simulations of the original system are compared and discussed.

**2.4. Numerical results from theoretical analysis.** On this section, the verification of the theoretical findings of the previous sections, with numerical simulations are shown.

A shaft with configuration, material, dimensions, that is following the Euler-Bernoulli beam assumptions, used in [2,3] is considered. It is a 1 m length ( $L$ ) shaft with internal and external radii  $r_i = 0.028$  m and  $r_o = 0.03$  m, respectively. It is made of stainless steel with the following material properties: density =  $7850 \text{ Kg/m}^3$ , Young's (shear) modulus  $E = 200 \text{ GPa}$  ( $G = 76.9 \text{ GPa}$ ), and Poisson's ratio  $\nu = 0.3$ , which leads to the following parameters:  $I_1 \cdot L = 12.04 \cdot 10^{-4} \text{ Kg} \cdot \text{m}$ ,  $F = 31.24 \cdot 10^{-3} \text{ m} \cdot \sqrt{\text{KG}}$ , and  $M = -41.55 \cdot 10^{-4}$ .

All the numerical results are mainly to confirm the theoretical analysis and identify its limitations. It should be highlighted that the initial angular position ( $\Theta_0$ ) can be arbitrarily defined since the origin of the fixed coordinates system that the angular initial position is related can have any orientation in space. The selected set of initial conditions for lateral bending motions corresponds to all instances with the same radial amplitude, obtained by combining the two deformations of the lateral bending motions.

Since this article is a review article, to make sense the findings of different publications, the best way is to start from the simple results and then move on to the more complex ones. Therefore, in the next subsection, before the examination of the normal modes solutions, the PMs solutions as rigid body modes of the spinning shaft numerically are examined. Then in the next subsection, the analytical findings relevant to other types of normal modes obtained through linearization around the PMs, that in many cases coincide with the 1<sup>st</sup> order approximation with numerical simulations are presented. Finally the validity of the multiple scales analysis with the existence of detuning frequencies in the dynamics of the spinning shaft, in the third numerical subsection is shown.

**Numerical results confirming rigid body motions on PMs.** The following 3-sets of initial conditions (ICs), associated with each one of the three perpetual manifolds, are considered:

-The 1<sup>st</sup> set of ICs associated with the 1<sup>st</sup> PM (eq. 34a),

$(q_{0,v}, q_{0,w}, q_{0,\phi}, \dot{\theta}_0, \dot{q}_{0,v}, \dot{q}_{0,w}, \dot{q}_{0,\phi}) = (0,0,0,10,0,0,0)$ , and corresponds to a period  $T_1 = 0.6283 \text{ s}$ , as given by (eq. 35c).

-The 2<sup>nd</sup> set of ICs associated with the 2<sup>nd</sup> PM (eq. 34b),

$(q_{0,v}, q_{0,w}, q_{0,\phi}, \dot{\theta}_0, \dot{q}_{0,v}, \dot{q}_{0,w}, \dot{q}_{0,\phi}) = (8,10,0,1022.16,0,0,0)$ , and corresponds to a period  $T_2 = 0.0061 \text{ s}$ .

-The 3<sup>rd</sup> set of ICs associated with the 3<sup>rd</sup> PM (eq. 34c),

$(q_{0,v}, q_{0,w}, q_{0,\phi}, \dot{\theta}_0, \dot{q}_{0,v}, \dot{q}_{0,w}, \dot{q}_{0,\phi}) = (0,0,5,4916.41,0,0,0)$ , and corresponds to a period  $T_3 = 0.0013 \text{ s}$ .

The initial angular position ( $\Theta_0$ ) is selected to be zero.

In Figures 3a-c, the numerically determined transient responses, of equations (9) are depicted. The transient responses obtained with initial conditions associated with the 1<sup>st</sup> PM in Figure (3a) are depicted, with only rigid body angular ( $\Theta$ ) motion and period  $T_1 = 0.6283 \text{ s}$  which is the same as the analytically defined period of the rigid body angular

motion. In Figure (3b) the transient responses associated with the 2<sup>nd</sup> PM are depicted. Examination indicates only rigid body angular motion with fixed lateral bending deformation and the same as the analytically defined period of  $T_2 = 0.0061$  s. Finally, the 3<sup>rd</sup> PM initial conditions lead to the transient responses depicted in Figure (3c). There is only rigid body angular periodic motion with fixed torsional ‘modal’ deformation with period of  $T_3 = 0.0013$  s, which is the same as the analytical value.

**Numerical results confirming normal modes solutions defined by perpetual manifolds.** The validity of the four theoretically determined normal modes obtained with linearization around the PMs of §2.3, through numerical simulations is discussed on this subsection.

Based on the parameters defining the spinning shaft configuration, in Table 1, the characteristic values on the spinning shaft dynamics are presented. The two characteristic values of the angular velocities that define the 2<sup>nd</sup>  $\omega_b \cdot \sqrt{1-M}$  and the 3<sup>rd</sup> PM ( $\omega_T$ ), and the characteristic value of the angular velocity  $\omega_b \cdot (1-M)/\sqrt{-M}$  that in the 1<sup>st</sup> PM the eigenvalues for lateral bending motions are qualitatively changing from pure imaginary to complex with nonzero real parts. Also, the characteristic values determining the normal modes (periodic motions) of the system, obtained by the linearization around the perpetual manifolds, are shown.

Considering the 1<sup>st</sup> PM, there are 3 normal modes associated with particular critical speeds, one for torsional motion ( $\dot{\theta}_{0,T,cr,1}$ ) and two for lateral bending motion ( $\dot{\theta}_{0,B,cr,j}$  with  $j = 1,2$ ). All of them coincide with the 1<sup>st</sup> order approximation of multiple scales analysis without considering the amplitude modulation equations.

In Table 1 is clear that the qualitative change of the eigenvalues describing lateral bending motions  $\omega_b \cdot (1-M)/\sqrt{-M}$  corresponds to much higher angular velocities than these that correspond to normal modes ( $\dot{\theta}_{0,B,cr,j}$  with  $j = 1,2$ ).

The fourth normal mode is obtained by the linearization of the 3<sup>rd</sup> PM, with angular velocity equal to the torsional characteristic frequency ( $\omega_T$ ), and the torsional modal displacement ( $q_{\phi,cr}$ ) as by the equation (6) is defined, and in Table 1 is indicated. Noting that this normal mode cannot easily obtained from the multiple scale analysis, therefore forms add-on information provided by the PMs approach.

TABLE 1. Characteristic values on the dynamics of the spinning shaft based on solutions around the PMs [3].

$\frac{\omega_b}{\sqrt{1-M}}$	$\omega_T$	$\frac{\omega_b \cdot (1-M)}{\sqrt{-M}}$	$\dot{\theta}_{0,T,cr,1}$	$\dot{\theta}_{0,B,cr,1}$	$\dot{\theta}_{0,B,cr,2}$	$q_{\phi,cr} \times 10^4$
(rad/s)/ (R.P.M.)	(rad/s)/ (R.P.M.)	(rad/s)/ (R.P.M.)	(rad/s)/ (R.P.M.)	(rad/s) / (R.P.M.)	(rad/s) / (R.P.M.)	rad · m · $\sqrt{Kg}$ (for $\omega_T$ )
1022.16/ 9761	4916.41/ 46948	15890.24/ 151741	4507.95/ 43048	510.82/ 4878	15857.33/ 151426	87.21

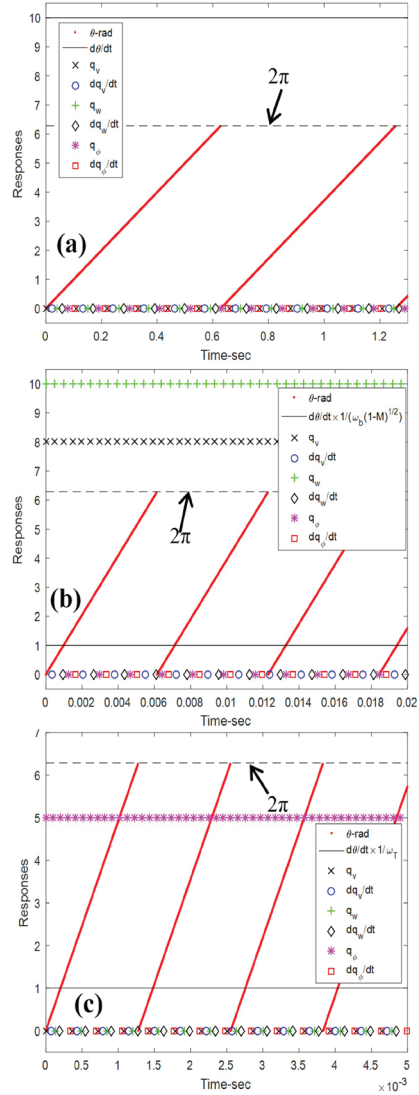


FIGURE 3. Numerically determined transient responses, (a) with the 1<sup>st</sup> set of initial conditions, (b) with the 2<sup>nd</sup> set of the initial conditions and, (c) with the 3<sup>rd</sup> set of initial conditions [3].

The theoretical analysis of normal modes in two sets of numerical simulations is presented. The 1<sup>st</sup> set considers only the linearization around the PMs/1<sup>st</sup> order approximation of multiple scales analysis neglecting the detuning frequencies, and the 2<sup>nd</sup> set considering also the amplitude modulation equations.

In [2], the Campbell diagram for lateral bending motions obtained from FEA (ANSYS) and incorporating the analytical results is examined. More precisely, the

analytical frequencies ( $f_i$ , for  $j = 1, 2$ ) obtained from the first-order approximation, neglecting the detuning frequencies, are in good agreement with those obtained from FEA, and the critical speed is on 4878 R.P.M. ( $\dot{\theta}_{0,B,cr,1}$ ), which is validating the 1<sup>st</sup> order approximation analysis and the PPs linearization analysis presented herein, that are associated with the steady states of the spinning shaft.

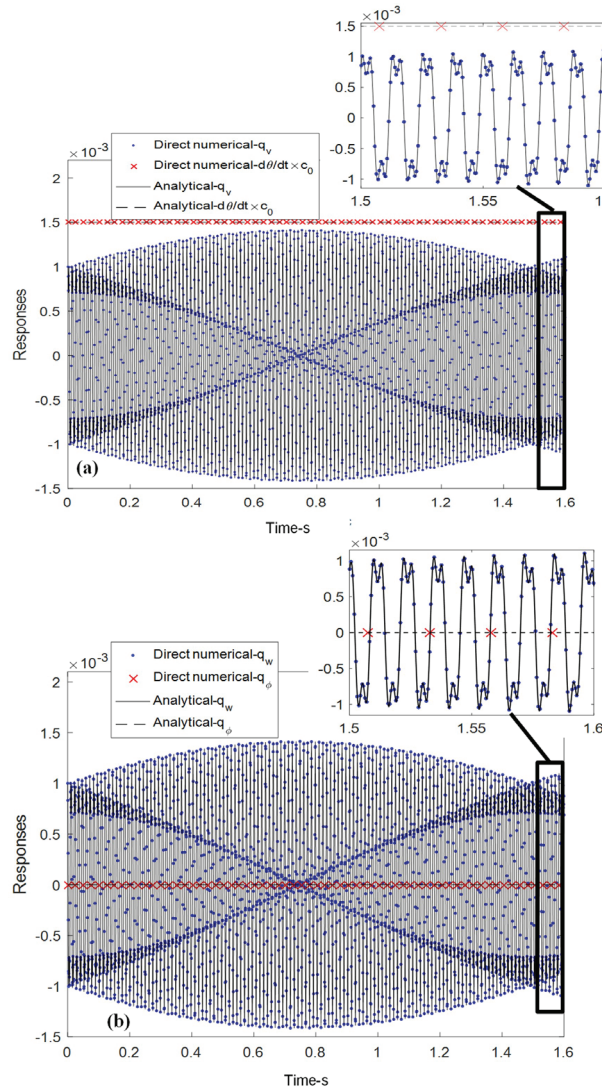


FIGURE 4. Transient responses at first critical speed  $\dot{\theta}_{0,B,cr,1}=510.82$  rad/s. a) rigid body angular velocity  $-\dot{\theta}$  and the lateral bending modal displacement  $-q_v$  with  $c_0 = 2.9365 \times 10^{-6}$ , b) torsional 'modal' displacement  $-q_\phi$  and the lateral bending modal displacement  $-q_w$  [3].

*Transient responses of normal modes for lateral bending motion*

Normal modes for lateral bending motion, identified only around 1<sup>st</sup> PM for two critical speeds as in Table 1 are shown.

Firstly, a perturbation of the 1<sup>st</sup> PM, for  $\dot{\theta}_{0,B,cr,1}$  (=510.82 rad/s), with initial conditions of  $(q_{0,v}, q_{0,w}) = (\xi_{0,1}, \xi_{0,2}) = (10^{-3}, 10^{-3})$  and the rest of the perturbations being zero, is considered. This perturbation is resulting 1.2 mm radial initial deformation of the shaft [3]. In Figures 4a-b, the transient responses obtained from direct numerical simulations of equations (9), and those defined by the analytical solution eqs (A.1a-b) and (A.20a-b) [3]. In Figure 4a, the analytically, and the numerically determined rigid body angular velocity  $-\dot{\theta}$  and lateral bending modal displacement  $-q_v$ , are depicted, and they are in very good agreement. The rigid body angular velocity is constant. Figure 4b, depicts, the torsional 'modal' displacement  $-q_\phi$  and the lateral bending modal displacement  $-q_w$  numerically and analytically determined. The numerical with the analytical results are in very good agreement.

Considering the 2<sup>nd</sup> critical speed  $\dot{\theta}_{0,B,cr,1}$  (=15857.33 rad/s), the analytical solution eqs (A.1a-b) and (A.20a-b), even for very small values of perturbations, is in high disagreement with the numerical simulations, as in [3] is shown.

*Transient responses of normal modes for torsional motion*

Two normal modes identified in torsion, the first one arises with perturbation of 1<sup>st</sup> PM and the 2<sup>nd</sup> normal mode arises with perturbation of the 3<sup>rd</sup> PM.

The first normal mode for small deformations (for the validity of 1<sup>st</sup> order approximation) is defined, and for angular velocity  $-\dot{\theta}_{0,T,cr,1}$  (=4507.95 rad/s). Perturbation of torsional modal angle  $q_{0,\phi} = \xi_{0,3} = 10^{-3}$  is considered and the rest of the perturbations being zero. In Figure 5, the transient responses obtained from direct numerical simulations of equation (9) and the analytical solutions given by equations (A.1a-b and A.20a-b), are depicted [3]. In Figure 5a, the torsional 'modal' displacements are depicted and the numerical results are in very good agreement with the numerical. The numerically determined lateral bending modal displacements are in very good agreement with the analytically determined, shown in Figure 5b. This is a torsional normal mode, with the lateral bending modal displacements coalescence as Figure 5b is shown. In Figure 5c the numerically and the analytically determined rigid body angular velocity, are depicted, and they are in very good agreement.

The 2<sup>nd</sup> normal mode in torsion arise by the 3<sup>rd</sup> PM,  $\dot{\theta}_0(0) = \omega_T + \xi_{3,4}(0) = 4906.41$  rad/s ( $\xi_{3,4}(0) = -10$  rad/s), torsional angle  $q_\phi(0) = \gamma_{0,3,cr} + \xi_{3,3}(0) = 0.009721$  ( $\xi_3(0) = 10^{-3}$ ), and a large perturbation of angular velocity  $q_\phi(0) = \xi_{3,7}(0) = 0.1$ . In Figures 6a-d, the transient responses obtained from direct numerical integration of equation (9) are depicted, incorporating those obtained by the equations (56a-b), (57) and (A.20a-d), and they are in very good agreement. In Figure 6a, the torsional 'modal' displacement is depicted, and seems that it is an unstable motion, since for the first time instances, the numerical responses are coincide with the analytical ones. However, after some cycles of oscillations the numerical solution is deviating from the analytical solution. Figure 6b depicts, the two modal lateral bending displacements, they are coalescence,

and there is a good agreement between the numerical with the analytical results. In Figure 6c the torsional modal velocities are depicted, the good agreement between the numerical with the analytical results in early stages is obvious, and the instability of this normal mode is further confirmed. In Figure 6d the rigid body angular velocity is depicted, and similarly in early stages there is agreement between numerical with analytical results and then their disagreement due to the instability of the normal mode is becoming profound.

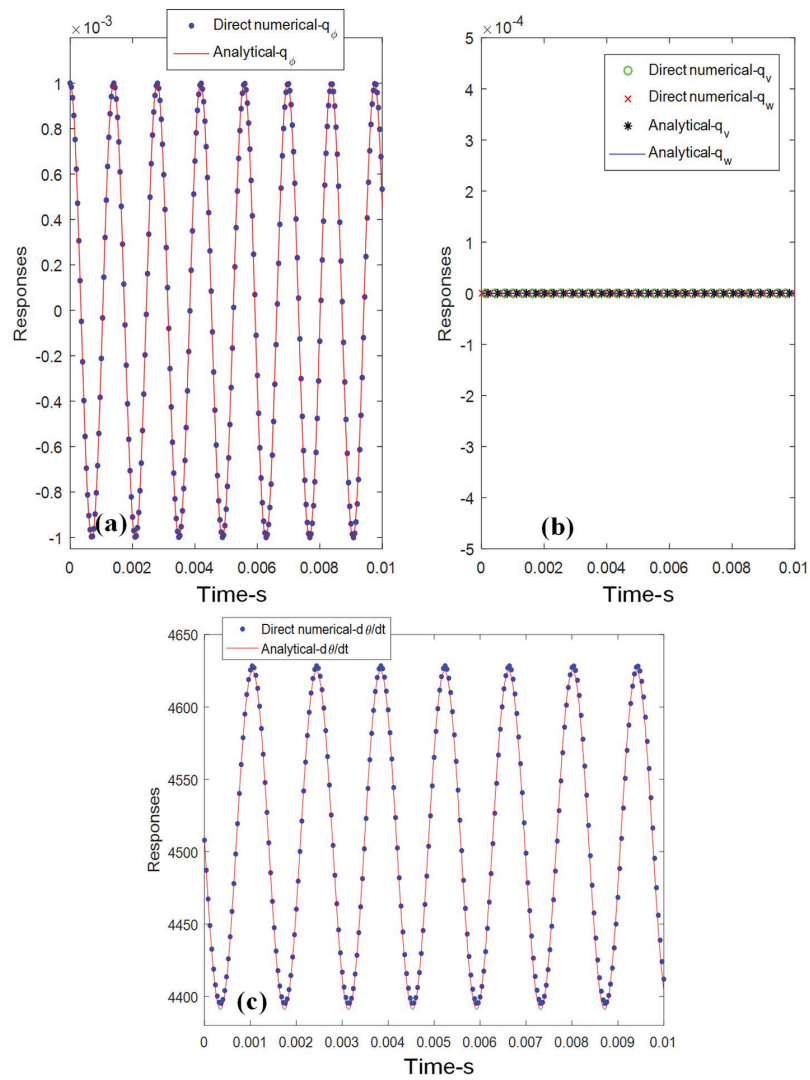


FIGURE 5. Transient responses for torsional critical speed  $\dot{\theta}_{0,Tcr,1,2}=4507.95$  rad/s, a) torsional angle  $-q_\phi$ , b) lateral bending motions  $q_v$  and  $q_w$ , c) angular velocity  $-\dot{\theta}$  [3].

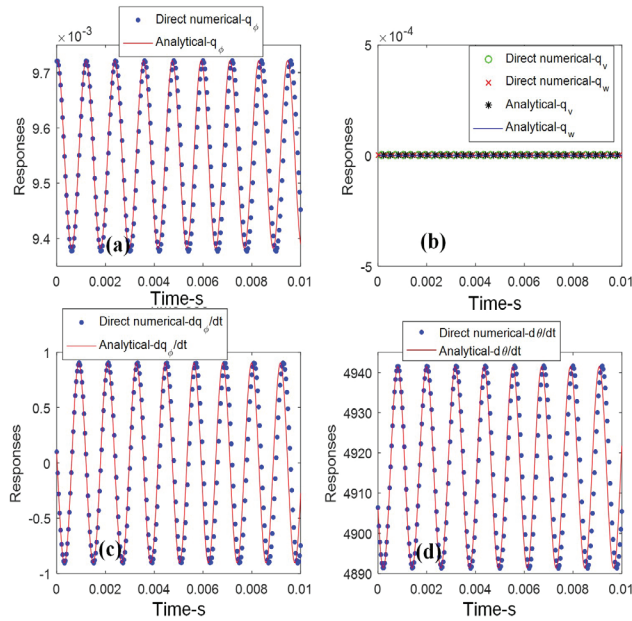


FIGURE 6. Transient responses for torsional normal mode of the linearized system of the 3rd family of equilibrium points with  $\dot{\theta}_0 = 4906.41$  rad/s, torsional angle  $q_\phi = 0.009721$  and torsional velocity  $\dot{q}_\phi = 0.1$ . a) torsional angle  $-q_\phi$ , b) lateral bending motions  $q_v$  and  $q_w$ , c) torsional velocity  $-\dot{q}_\phi$ , and d) angular velocity  $-\dot{\theta}$  [3].

### Numerical results confirming the solutions from multiple time scales analysis.

On this subsection the multiple scales nonlinear dynamic analysis, through numerical simulations is discussed.

In [2] numerical simulations, 4 angular velocities considered, but only for small angular velocity with value  $\dot{\theta}_a(0) = 104.72$  rad/s (=1000 R.P.M.) there is a confirmation of the analytical results. The following set of initial conditions considered,

$$q_v(0) = 1, q_w(0) = 1, \dot{q}_v(0) = 0, \dot{q}_w(0) = 0, q_\phi(0) = 0, \dot{q}_\phi(0) = 0. \quad (74)$$

The above initial conditions resulting a very high initial deformation but it is a good set for examining the theoretical analysis.

In Figure 7, the numerically obtained responses are depicted, incorporating the analytical solutions obtained from a) 1<sup>st</sup> order approximation without detuning frequencies, equations (A.1a-b) and (A.20a-b) and b) 1<sup>st</sup> order approximation with detuning frequencies given by equations (A.8a-b), (A.27a-b).

In lateral bending motions (fig. 7a-b) the 1<sup>st</sup> order approximation with the detuning frequencies are in very good agreement with the numerical solution, since the detuning frequencies are not zero the 1<sup>st</sup> order approximation without detuning

frequencies is not capturing the dynamics. The torsional ‘modal’ displacement and rigid body angular velocity are approximated as an envelope without capturing the numerical simulation’s details, as in Figure 7c-d, are depicted.

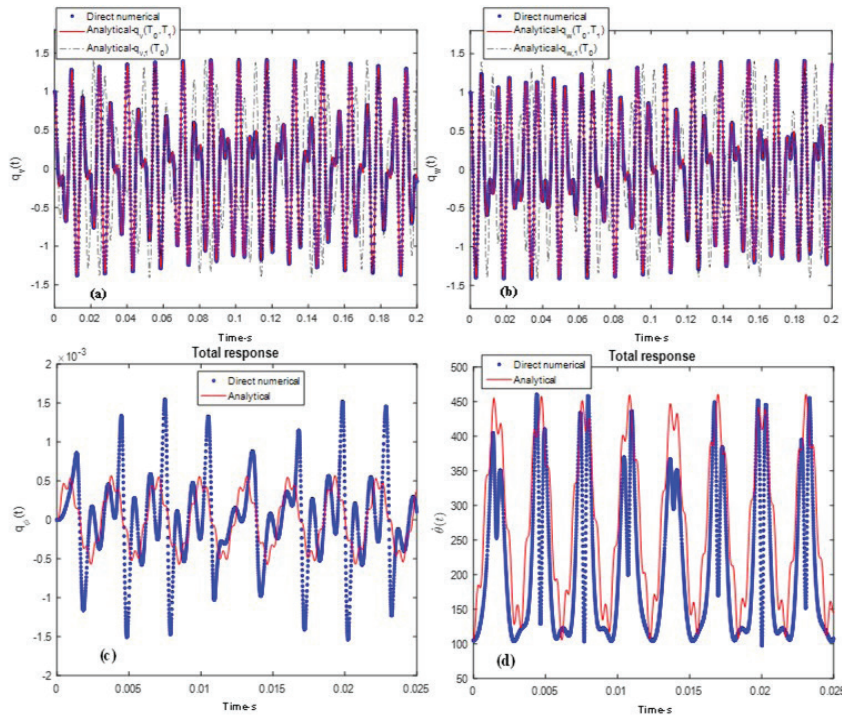


FIGURE 7. Comparison of the direct numerical integration responses with the multiple scales solution for  $\dot{\theta}_a(0) = 104.72$  rad/sec: a) bending motion in y-direction ( $q_v(t)$ ), b) bending motion in z-direction ( $q_w(t)$ ), c) torsional modal angle ( $q_\phi(t)$ ) and, d) angular velocity ( $\dot{\theta}(t)$ ) [2].

Highlighting that the numerical simulation presented herein is for 1000 R.P.M, which is much smaller from the 1<sup>st</sup> and 2<sup>nd</sup> critical speeds. Therefore further analysis is needed for identifying the detuning frequencies in critical situations for the spinning shaft.

**2.5. Discussion of this section.** On this section nonlinear dynamic analysis of a spinning shaft with non-constant rotating speed, with two ways, has been presented. The system of equations describing the motion as highlighted in [4], is a system with zero eigenvalues associated with the underlying linear system, and they are associated with rigid body modes. In this case, the Lyapunov solutions, in low energies the nonlinear system’s dynamics, is described by the underlying linear modes is not necessarily valid. Therefore the methods with development relying to the underlying linear modes most likely cannot provide accurate results. Typical practice in discrete systems with rigid

body modes is a change of variables such that the system becomes 'grounded' in one of the generalized coordinates, and the rigid body modes are disappearing. In our system, the original equations are PDEs. The 'grounding' in one of the deformation variables makes the system very complicated, e.g. the torsional deformation with rigid body motion, leading to coupling of the lateral bending with torsional motion, through the Coriolis and the centrifugal forces.

The 1<sup>st</sup> method of nonlinear dynamic analysis, is the well-established multiple scales analysis, and herein the results arose by incorporating two time scales with detuning frequencies from the steady states solutions.

The 2<sup>nd</sup> approach was performed with linearization around the PMs that form the backbone lines of rigid body modes. The analytical results obtained with the linearization around the 1<sup>st</sup> PM, overlap with the analytical results obtained with the 1<sup>st</sup> order approximation from the multiple-scale analysis. The combination of the 3 PMs of rigid body modes, and the eigenvalues associated with the dynamical systems arising from the linearization of the original system around the PMs, leads to several observations. In a plot that is the projection of the backbone lines, of the rigid body motions of the spinning shaft with non-constant rotating speed, to 3D make some things very clear. There is qualitative change of the eigenvalues, for different values of the angular velocity associated with the linear systems around 1<sup>st</sup> PM, and leads to trajectories associated with variant Lyapunov exponents and chaotic motions.

Moreover four sets of normal modes that define critical situations have been determined. The three of them coincide with multiple scale analysis. The fourth one is a torsional normal mode that through the PMs linearization can directly obtained.

Apart of the normal modes, that define the critical situations, the regions in the backbone lines of rigid body modes with the dynamical systems associated with eigenvalues having positive real parts, means that the solutions are escape to infinity, and this form another type of critical situations, that can be examined further on.

Although the mathematical analysis is extensive, the definition of the critical situations, of the spinning shaft with non-constant rotating speed, needs more work, for the definition of the normal modes e.g. away from the PMs and in the regions that the dynamics is described by linear dynamical systems associated with eigenvalues with positive real parts.

Also, the full chaotic motions analysis is still incomplete, e.g. the determination of the basins of attraction, and therefore further work is needed.

The above mentioned nonlinear dynamic analysis through the observation that the PPs are associated with the rigid body modes paved the way for developing the theorems presented in the subsequent sections.

### 3. Theorems in mechanics about rigid body motions

**3.1. Theorems about perpetual points of mechanical systems.** The first analysis of determining the spinning shaft's perpetual points leads to a preliminary conclusion that the perpetual points are associated with rigid body motions in mechanical systems. Later on, simpler mechanical systems have been examined to verify it. In Figure 8, the configuration of a 2 degrees of freedom mechanical system is shown.

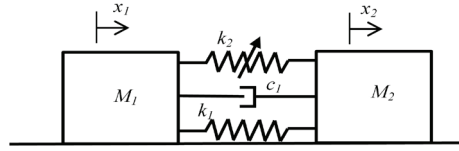


FIGURE 8. Configuration of the 2 degrees of freedom mechanical system.

The equations of motion are given by,

$$M_1 \cdot \ddot{x}_1 + k_1 \cdot (x_1 - x_2) + k_2 \cdot (x_1 - x_2)^3 + c_1 \cdot (\dot{x}_1 - \dot{x}_2) = 0, \tag{75a}$$

$$M_2 \cdot \ddot{x}_2 - k_1 \cdot (x_1 - x_2) - k_2 \cdot (x_1 - x_2)^3 - c_1 \cdot (\dot{x}_1 - \dot{x}_2) = 0, \tag{75b}$$

and taking their derivative in time the following equations of jerks arise,

$$M_1 \cdot \dddot{x}_1 + k_1 \cdot (\dot{x}_1 - \dot{x}_2) + 3 \cdot k_2 \cdot (x_1 - x_2)^2 \cdot (\dot{x}_1 - \dot{x}_2) + c_1 \cdot (\ddot{x}_1 - \ddot{x}_2) = 0, \tag{76a}$$

$$M_2 \cdot \dddot{x}_2 - k_1 \cdot (\dot{x}_1 - \dot{x}_2) - 3 \cdot k_2 \cdot (x_1 - x_2)^2 \cdot (\dot{x}_1 - \dot{x}_2) - c_1 \cdot (\ddot{x}_1 - \ddot{x}_2) = 0. \tag{76b}$$

The perpetual points of this system, by setting jerks and accelerations to zero, in [8] are determined, and they are given by,

1<sup>st</sup> set,

$$U_{2-dof} = \{(x_2, \dot{x}_2, \ddot{x}_2, \ddot{x}_2), (x_2, \dot{x}_2) \in \mathbb{R} \times \mathbb{R}^*\}, \tag{77a}$$

2<sup>nd</sup> set,

$$S_{2-dof} = \left\{ \left( x_2 \pm \sqrt{-\frac{k_1}{k_2}}, x_2, \dot{x}_2, \dot{x}_2 \right), (x_2, \dot{x}_2) \in \mathbb{R} \times \mathbb{R}^*, k_1 \in \mathbb{R}_{>0}, k_2 \in \mathbb{R}_{<0} \right\}, \tag{77b}$$

3<sup>rd</sup> set,

$$W_{2-dof} = \left\{ \left( x_2 \pm \sqrt{-\frac{k_1}{3 \cdot k_2}}, x_2, \dot{x}_2 \mp \frac{2 \cdot k_1}{3 \cdot c_1} \cdot \sqrt{-\frac{k_1}{3 \cdot k_2}}, \dot{x}_2 \right), (x_2, \dot{x}_2) \in \mathbb{R} \times \mathbb{R}^*, \right. \\ \left. k_1 \in \mathbb{R}_{>0}, k_2 \in \mathbb{R}_{<0}, c_1 \in \mathbb{R}^* \right\}, \tag{77c}$$

Since in all sets the generalized coordinates can have any real value and the generalized velocities any non-zero real value, they are infinite points and they are forming manifolds in state space, the perpetual manifolds [8]. The two first sets are associated with rigid body motions.

In case that the system is linear ( $k_2 = 0$ ), only the first set of perpetual points exists as in [7] without damping ( $c_1 = 0$ ) and in [8] with damping ( $c_1 \neq 0$ ), are shown. In considering nonlinearities but without damping ( $c_1 = 0$ ), only the 1<sup>st</sup> and the 2<sup>nd</sup> sets of perpetual points exist and they are associated with rigid body motions [7].

The 2<sup>nd</sup> set of perpetual points, extended to N-Degrees of Freedom (dof) systems,

$$S = \{(q_1(t), \dots, q_N(t), \dot{q}_s, \dots, \dot{q}_s), (q_1(t), \dots, q_N(t), \dot{q}_s) \in \mathbb{R}^N \times \mathbb{R}^*\}, \tag{78a}$$

is forming the perpetual manifolds of rigid body motions [9], that all the inertia elements are moving with constant not necessarily zero distance with the same velocities.

The 1<sup>st</sup> set of perpetual points, extended to N-dof systems,

$$U = \{(q_s(t), \dots, q_s(t), \dot{q}_s, \dots, \dot{q}_s), (q_s(t), \dot{q}_s) \in \mathbb{R} \times \mathbb{R}^s\}, \quad (78b)$$

is forming the perpetual manifolds of exact rigid body motions [9].

In [7], the following theorem about the perpetual points of conservative linear natural mechanical systems proved:

**THEOREM 1.** *The perpetual points in linear conservative natural mechanical systems are defined by the rigid body motions and the inverse. [7]*

In [8], for dissipative linear natural mechanical systems, another theorem proved and stated:

**THEOREM 2.** *The perpetual points in linear natural mechanical discrete systems with viscous damping excepting any externally applied load, are defined by the rigid body motions and they exist if both stiffness and damping matrices are positive semi-definite. [8]*

And,

**INVERSE OF THEOREM 2.** *The rigid body motions define the perpetual points in linear natural mechanical discrete systems with viscous damping excepting any externally applied load, if and only if the damping matrix is positive semi-definite. [8]*

The connection of perpetual points of mechanical systems with their rigid body motions leads to some definitions in mechanics and the proof of a theorem, that in the following section, is presented.

**3.2. Definitions of perpetual mechanical systems, augmented perpetual manifolds, and a relevant theorem with a corollary.** The main observation that the perpetual points are associated with rigid body motions, that whereas exist on the mechanical systems, lead to the preliminary idea, as stated in the conclusions of [7], that the perpetual points formalism can be used for exciting only the rigid body modes, without any oscillations.

Recalling in mathematical terms the definition of perpetual points of a mechanical system,

$$\ddot{q}_1 = \ddot{q}_2 = \dots = \ddot{q}_N = 0, \quad (79a)$$

and,

$$\ddot{\ddot{q}}_1 = \ddot{\ddot{q}}_2 = \dots = \ddot{\ddot{q}}_N = 0, \quad (79b)$$

leads to the following question:

Is it possible only the left-hand side of these equations (79a-b) to be valid by means without necessarily being zero or constant accelerations?

The question's address leads to developing the framework in [10] and [9] for triggering rigid body modes, or otherwise stated external excited flexible N-dof systems to move as rigid body without any oscillations. In [10], the description of

some definitions are written, that they are mathematically strictly defined in [9]. Moreover, the theorem's statement in [10] is written, and in [9] is proved.

**Definition of Perpetual Mechanical Systems.** A discrete dissipative mechanical system, without any external forcing that is described by the following equations of motion,

$$\begin{aligned} & [\mathbf{M}_{ij}(t, q_l(t), \dot{q}_m(t))] \times \{\ddot{q}_i(t)\} + [\mathbf{C}_{ij}] \times \{\dot{q}_i(t)\} + \\ & + [\mathbf{K}_{ij}] \times \{q_i(t)\} + \{\mathbf{F}_{NL,i}(q_n(t), \dot{q}_o(t))\} = \{0\}, \text{ for} \\ & i = 1, \dots, N, j = 1, \dots, N, l, m, n, o \in \{1, 2, \dots, N\}, \text{ and} \\ & (q_i(t), \dot{q}_i(t), \ddot{q}_i(t)) \in \mathbb{R}^3, \end{aligned} \quad (80)$$

whereas,

$[\mathbf{M}_{ij}(t, q_l(t), \dot{q}_m(t))]$  is a real  $N \times N$  state-dependent matrix with elements that may be nonsmooth and nonlinear functions, and nonzero all the sums of rows,

$[\mathbf{K}_{ij}]$  and  $[\mathbf{C}_{ij}]$ , are real  $N \times N$  constant, stiffness and proportional to velocity vector, matrices, respectively,

$\{\mathbf{F}_{NL,i}\}$ , is a  $N \times 1$  vector with elements state-dependent nonlinear functions which can also be nonsmooth but singled valued for rigid body motions,

is called discrete **Perpetual Mechanical System** if admits as perpetual points the exact perpetual manifolds of rigid body motions. [9]

**Definitions of Augmented Perpetual Manifolds.** The  $2N + 1$  dimensional **Augmented Perpetual Manifolds**, e.g.,  $M_a$  of an  $N$ -dof mechanical discrete system, with generalized coordinates  $q_i$  that admits solutions of perpetual manifolds arise when,

$$\ddot{q}_i(t) = \ddot{q}_a(t), \quad \text{for } i = 1, \dots, N, \text{ and } \ddot{q}_a(t) \in \mathbb{R}, \quad (81)$$

and the solutions of the system in state space, define them, as,

$$\begin{aligned} M_a = \{ & (t, q_{a,1}(t) + c_1 \cdot (t - t_0) + d_1, \dots, q_{a,N}(t) + c_N \cdot (t - t_0) + d_N \\ & \dot{q}_{a,1}(t) + c_1, \dots, \dot{q}_{a,N}(t) + c_N): \\ & (t, q_{a,i}(t), \dot{q}_{a,i}(t)) \in \mathbb{R}^{2 \cdot N + 1}, (c_1, \dots, c_N, d_1, \dots, d_N) \in \mathbb{R}^{2 \cdot N}\}, \end{aligned} \quad (82a)$$

whereas the constants are given by considering the initial conditions as follows,

$$\dot{q}_i(t_0) = \dot{q}_{a,i}(t_0) + c_i, \quad \text{for } i = 1, \dots, N, \quad (82b)$$

and,

$$q_i(t_0) = q_{a,i}(t_0) + d_i, \quad \text{for } i = 1, \dots, N. \quad (82c) \text{ [9]}$$

Further on, in case that the constants  $-c_i$  ( $i = 1, \dots, N$ ) in equation (82a) are equal to zero, lead to the augmented perpetual manifolds, e.g.,  $W_a$  of rigid body motions, which are given by,

$$\begin{aligned} W_a = \{ & (t, q_{a,1}(t) + d_1, \dots, q_{a,N}(t) + d_N, \dot{q}_a(t), \dots \\ & \dot{q}_a(t)): (t, q_{a,i}(t), \dot{q}_a(t)) \in \mathbb{R}^{N+2}, (d_1, \dots, d_N) \in \mathbb{R}^{2 \cdot N}\}. \end{aligned} \quad (83)$$

In the augmented perpetual manifolds of rigid body motion, each part of the system moves together with the rest of the system, maintaining not necessarily zero but a constant distance of the relative positions. [9]

In case that all the constants  $-c_i, d_i$  ( $i = 1, \dots, N$ ), in equation (82a) are equal to zero, then the augmented perpetual manifolds of rigid body motions are called **Exact Augmented Perpetual Manifolds** ( $X_a$ ), which are given by,

$$X_a = \left\{ (t, q_a(t), \dots, q_a(t), \dot{q}_a(t), \dots, \dot{q}_a(t)) : (t, q_a(t), \dot{q}_a(t)) \in \mathbb{R}^3 \right\}. \quad (84) [9]$$

In the exact augmented perpetual manifolds, the system is moving like a particle.

After the definition of the exact augmented perpetual manifolds the proof of the following theorem, is straightforward as in [9] is shown.

**THEOREM 3.** Any  $N(\geq 2)$ -degrees of freedom discrete mechanical system with generalized coordinates  $q_i(t)$  that can be written as a perpetual mechanical system with external forcing that is described by the following system of differential equations,

$$\begin{aligned} & [\mathbf{M}_{i,j}(t, q_l(t), \dot{q}_m(t))] \times \{\ddot{q}_i(t)\} + [\mathbf{C}_{i,j}] \times \{\dot{q}_i(t)\} + [\mathbf{K}_{i,j}] \times \{q_i(t)\} + \\ & + \{\mathbf{F}_i^{NL}(q_n(t), \dot{q}_o(t))\} = \{\mathbf{F}_i(t, q_p(t), \dot{q}_q(t))\}, \text{ for} \\ & i = 1, \dots, N, j = 1, \dots, N, l, m, n, o, p, q \in \{1, 2, \dots, N\}, \\ & (q_i(t), \dot{q}_i(t), \ddot{q}_i(t)) \in \mathbb{R}^3, \end{aligned} \quad (85)$$

and admits unique solutions for the following matrices,

$[\mathbf{M}_{ij}]$  is a real  $N \times N$  inertia matrix with elements that can be, nonsmooth, nonlinear, time and state dependent, functions but having at least one nonzero sum of  $k$ -row for all time instants,

$[\mathbf{K}_{ij}]$  and  $[\mathbf{C}_{ij}]$ , are real  $N \times N$  constant, stiffness and proportional to velocity vector, matrices,

$\{\mathbf{F}_i^{NL}\}$  is a  $N \times 1$  vector of nonlinear internal forces with elements state dependent nonlinear functions which can be nonsmooth but single-valued for rigid body motions, and  $\mathbf{F}_i^{NL}(q_s, 0) = 0$  for  $q_s \in \mathbb{R}$ ,

$\{\mathbf{F}_i\}$  is a real  $N \times 1$  vector of external forces with elements, time and state dependent, maybe nonlinear and nonsmooth functions,

if the external forces ( $F_j$ ) with the reference  $k$ -inertia external force ( $F_k$ ) are related as follows,

$$F_i(t, q_a(t), \dot{q}_a(t)) = \frac{\sum_{j=1}^N M_{i,j}(t, q_a(t), \dot{q}_a(t)) \cdot F_k(t, q_a(t), \dot{q}_a(t))}{\sum_{j=1}^N M_{k,j}(t, q_a(t), \dot{q}_a(t))}, \text{ for} \\ i, k \in \{1, 2, \dots, N\}, \text{ and } q_a(t) = q_i(t), \dot{q}_a(t) = \dot{q}_i(t), \quad (86)$$

then, the solution of any of the following differential equations,

$$\ddot{q}_a(t) = \frac{F_k(t, q_a(t), \dot{q}_a(t))}{\sum_{j=1}^N M_{k,j}(t, q_a(t), \dot{q}_a(t))} = G(t, q_a(t), \dot{q}_a(t)), \quad (87)$$

with vector field  $G$ , for the following set of initial conditions at the time instant  $t_0$ ,

$$q_i(t_0) = q_a(t_0), \text{ for } i = 1, \dots, N, \text{ and, } q_a(t_0) \in \mathbb{R}, \tag{88a}$$

$$\dot{q}_i(t_0) = \dot{q}_a(t_0), \text{ for } i = 1, \dots, N, \text{ and, } \dot{q}_a(t_0) \in \mathbb{R}, \tag{88b}$$

is defining the generalized coordinates  $-q_i$  and their velocities in the exact augmented perpetual manifold,

$$X_a = \{(t, q_a(t), \dots, q_a(t), \dot{q}_a(t), \dots, \dot{q}_a(t)), (t, q_a(t), \dot{q}_a(t)) \in \mathbb{R}^3\}. \tag{89} [9-10]$$

After the above theorem the following corollary in [9] is stated and proved.

**COROLLARY.** In an externally forced discrete perpetual mechanical system, if the exact augmented perpetual manifold is formed, by a harmonic motion, even though the system is flexible, the system behaves in dual mode as a wave-particle. [9]

**Example for the analytical and the numerical verification of the theorem.**

Herein the application of the theorem using the 1<sup>st</sup> example of [9] follows.

A 5-dof mechanical system is considered with the following equations of motion [9],

$$[M_{i,j}] \times \{\ddot{x}_i\} + [C_{i,j}] \times \{\dot{x}_i\} + [K_{i,j}] \times \{x_i\} + \{F_i^{NL}(x_n, \dot{x}_o)\} = \{F_{ext,i}(t)\}, \tag{90}$$

for  $n, o \in \{1, 2, \dots, 5\}, i = 1, \dots, 5$ .

The mass matrix is defined by [9],

$$[M_{i,j}] = \begin{bmatrix} m_1 & 0 & 0 & 0 & 0 \\ 0 & m_2 & 0 & 0 & 0 \\ 0 & 0 & m_3 & 0 & 0 \\ 0 & 0 & 0 & m_4 & 0 \\ 0 & 0 & 0 & 0 & m_5 \end{bmatrix}, \tag{91a}$$

with  $m_i$  ( $i = 1, \dots, 5$ ) being positive constants.

The stiffness matrix is given by [9],

$$[K_{i,j}] = \begin{bmatrix} k_1 & -k_1 & 0 & 0 & 0 \\ -k_1 & k_1 + k_2 & -k_2 & 0 & 0 \\ 0 & -k_2 & k_2 + k_3 & -k_3 & 0 \\ 0 & 0 & -k_3 & k_3 + k_4 & -k_4 \\ 0 & 0 & 0 & -k_4 & k_4 \end{bmatrix}. \tag{91b}$$

The damping matrix is given by [9],

$$[C_{i,j}] = \begin{bmatrix} c_1 & -c_1 & 0 & 0 & 0 \\ -c_1 & c_1 + c_2 & -c_2 & 0 & 0 \\ 0 & -c_2 & c_2 + c_3 & -c_3 & 0 \\ 0 & 0 & -c_3 & c_3 + c_4 & -c_4 \\ 0 & 0 & 0 & -c_4 & c_4 \end{bmatrix}. \tag{91c}$$

The nonlinear forces vector is [9],

$$\{F_i^{NL}(x_n, \dot{x}_o)\} = \left\{ \begin{array}{l} k_{nl,1} \cdot \sin(x_1 - x_2) \\ -k_{nl,1} \cdot \sin(x_1 - x_2) + k_{nl,2} \cdot (x_2 - x_3)^5 \\ -k_{nl,2} \cdot (x_2 - x_3)^5 + k_{nl,3} \cdot \sin(x_3 - x_4) \\ -k_{nl,3} \cdot \sin(x_3 - x_4) + k_{nl,4} \cdot (x_4 - x_5)^7 \\ -k_{nl,4} \cdot (x_4 - x_5)^7 \end{array} \right\} +$$

$$+ \left\{ \begin{array}{l} c_{nl,1} \cdot (\dot{x}_1 - \dot{x}_2)^3 \\ -c_{nl,1} \cdot (\dot{x}_1 - \dot{x}_2)^3 + c_{nl,2} \cdot (\dot{x}_2 - \dot{x}_3)^5 \\ -c_{nl,2} \cdot (\dot{x}_2 - \dot{x}_3)^5 + c_{nl,3} \cdot (\dot{x}_3 - \dot{x}_4)^7 \\ -c_{nl,3} \cdot (\dot{x}_3 - \dot{x}_4)^7 + c_{nl,4} \cdot \tanh(b \cdot (\dot{x}_4 - \dot{x}_5)) \\ -c_{nl,4} \cdot \tanh(b \cdot (\dot{x}_4 - \dot{x}_5)) \end{array} \right\}, \text{for } n, o \in \{1, 2, \dots, 5\}. \quad (91d)$$

The external forcing vector is [9],

$$\{\mathbf{F}_{ext,i}(t)\}^T = [1 \quad m_2/m_1 \quad m_3/m_1 \quad m_4/m_1 \quad m_5/m_1] \cdot F_{ext,1}(t). \quad (91e)$$

The system is fulfilling the theorem's conditions, and the solution the in exact augmented perpetual manifolds is given by [9-10],

$$\dot{x}_a(t) = \frac{F_{ext,1}(t)}{m_1}. \quad (92)$$

Two types of external forces considered in [9]:

1. Linear time-varying force ( $F_{ext,1}^{(1)}(t)$ ),

$$F_{ext,1}^{(1)}(t) = \eta \cdot t + c, \quad \text{with } (\eta, c) \in \mathbb{R}^2. \quad (93a)$$

The velocity ( $\dot{x}_a(t)$ ), is given by [9],

$$\dot{x}_{a,1}(t) = \frac{\eta}{2 \cdot \sum_{j=1}^N M_{k,j}} \cdot (t^2 - t_0^2) + \frac{c}{\sum_{j=1}^N M_{k,j}} \cdot (t - t_0) + \dot{x}_{a,1}(t_0), \quad (93b)$$

and the response ( $x_{a,1}(t)$ ), is given by [9],

$$\begin{aligned} x_{a,1}(t) &= \frac{\eta}{6 \cdot \sum_{j=1}^N M_{k,j}} \cdot (t^3 - t_0^3) + \frac{c}{2 \cdot \sum_{j=1}^N M_{k,j}} \cdot (t^2 - t_0^2) - \\ &- \left( \frac{\eta \cdot t_0^2}{2 \cdot \sum_{j=1}^N M_{k,j}} + \frac{c \cdot t_0}{\sum_{j=1}^N M_{k,j}} - \dot{x}_{a,1}(t_0) \right) \cdot (t - t_0) + x_{a,1}(t_0). \end{aligned} \quad (93c)$$

2. Single frequency harmonic forces ( $F_k^{(2)}$ ),

$$F_{ext,1}^{(2)}(t) = A_{ex} \cdot \sin(\omega_{ex} \cdot t + \theta_{ex}), \text{ with } (A_{ex}, \theta_{ex}) \in \mathbb{R}^2 \text{ and } \omega_{ex} \in \mathbb{R}_{\geq 0}, \quad (94a)$$

whereas,  $A_{ex}$  is the excitation amplitude, the external frequency and phase, are denoted as  $\omega_{ex}$  and  $\theta_{ex}$ , respectively. The velocity ( $\dot{x}_{a,2}(t)$ ) is given by [9],

$$\begin{aligned} \dot{x}_{a,2}(t) &= -\frac{A_{ex}}{\sum_{j=1}^N M_{k,j} \cdot \omega_{ex}} \cdot \cos(\omega_{ex} \cdot t + \theta_{ex}) + \\ &+ \frac{A_{ex} \cdot \cos(\omega_{ex} \cdot t_0 + \theta_{ex})}{\sum_{j=1}^N M_{k,j} \cdot \omega_{ex}} + \dot{x}_{a,2}(t_0), \end{aligned} \quad (94b)$$

and the response ( $x_{a,2}(t)$ ), is [9],

$$\begin{aligned} x_{a,2}(t) &= -\frac{A_{ex}}{\sum_{j=1}^N M_{k,j} \cdot \omega_{ex}^2} \cdot \sin(\omega_{ex} \cdot t + \theta_{ex}) + \\ &+ \left( \frac{A_{ex} \cdot \cos(\omega_{ex} \cdot t_0 + \theta_{ex})}{\sum_{j=1}^N M_{k,j} \cdot \omega_{ex}} + \dot{x}_{a,2}(t_0) \right) \cdot (t - t_0) + \\ &+ \frac{A_{ex} \cdot \sin(\omega_{ex} \cdot t_0 + \theta_{ex})}{\sum_{j=1}^N M_{k,j} \cdot \omega_{ex}^2} + x_{a,2}(t_0). \end{aligned} \quad (94c)$$

The form of equation (94c) is harmonic; with a wave solution in space. The wave velocity ( $wv$ ) is given by the last two terms of equation (94b) [9],

$$wv = \frac{A_{ex} \cdot \cos(\omega_{ex} \cdot t_0 + \theta_{ex})}{\sum_{j=1}^N M_{k,j} \omega_{ex}} + \dot{x}_{a,2}(t_0). \tag{94d}$$

The zero wave velocity leads to a standing wave motion, and the nonzero leads to a longitudinal wave motion. The 5 masses for this excitation force have the same displacements and the same velocities; therefore the system's motion with harmonic forcing is particle-wave motion.

TABLE 2. Values of the parameters forming the structural matrices [9].

$M_{i,j}$	$K_{i,j}$	$C_{i,j}$
$m_1 = 2000 \text{ kg}$	$k_1 = 1 \cdot 10^6 \text{ N/m}$	$c_1 = 1008.99 \text{ N} \cdot \text{s/m}$
$m_2 = 1000 \text{ kg}$	$k_2 = 1.4 \cdot 10^6 \text{ N/m}$	$c_2 = 1412.58 \text{ N} \cdot \text{s/m}$
$m_3 = 1500 \text{ kg}$	$k_3 = 1.3 \cdot 10^6 \text{ N/m}$	$c_3 = 1311.68 \text{ N} \cdot \text{s/m}$
$m_4 = 1200 \text{ kg}$	$k_4 = 1.2 \cdot 10^6 \text{ N/m}$	$c_4 = 1210.78 \text{ N} \cdot \text{s/m}$
$m_5 = 500 \text{ kg}$	–	–

TABLE 3. Values of the parameters of the nonlinear forces [9].

$F_i^{NL}$	
$k_{nl,1} = 1 \cdot 10^5 \text{ N}$	$c_{nl,1} = 1008.99 \text{ N} \cdot \text{s}^3/\text{m}^3$
$k_{nl,2} = -1.5 \cdot 10^5 \text{ N/m}^5$	$c_{nl,2} = 1412.58 \text{ N} \cdot \text{s}^5/\text{m}^5$
$k_{nl,3} = 1.3 \cdot 10^5 \text{ N}$	$c_{nl,3} = 1311.68 \text{ N} \cdot \text{s}^7/\text{m}^7$
$k_{nl,4} = 1.2 \cdot 10^5 \text{ N/m}^7$	$c_{nl,4} = 1210.78 \text{ N}$
–	–

TABLE 4. Initial conditions and the external forcing parameters [9].

$i$	Time interval (s)	ICs		External Forcing Parameters
		$\dot{x}_{a,i}(t_0)$ (m/s)	$x_{a,i}(t_0)$ (m)	
1	$t \in (0, 1]$	1	1	$\eta = 5000 \text{ N/s}$ $c = 10 \text{ N}$ $A_{ex,1} = -1.5867030608259 \cdot 10^5 \text{ N}$
2	$t \in (1, 2]$	2.255000	2.419167	$\omega_{ex} = 19.822 \text{ rad/s}$ $\theta_{ex} = 0 \text{ rad}$
3	$t \in (2, 3]$	2.440323	-1.461429	$A_{ex,2} = 2 \cdot 10^5 \text{ N}$ $\omega_{ex} = 19.822 \text{ rad/s}$ $\theta_{ex} = 0 \text{ rad}$

In the numerical simulations, the used values of the parameters, of the linear structural matrices, are in Table 2. The values of the parameters of the nonlinear forces are in Table 3. The external forcing parameters are in Table 4.

Figure 9a, depicts selected numerical displacements and the analytical solution, whereas the analytical solution is in good agreement with the numerical simulations. In first time interval from 0-1s, the system's motion is a rigid body curvilinear one, and later on wave-particle motion. More precisely in the 2<sup>nd</sup> time interval, from 1-2s, the motion is wave-particle with zero wave velocity. In the 3<sup>rd</sup> time interval, 2-3s, the motion is wave particle but with  $-3.303 \text{ m/s}$  wave velocity. Therefore, in the 2<sup>nd</sup> and the 3<sup>rd</sup> time intervals, the mechanical system moves in dual mode, as wave-particle.

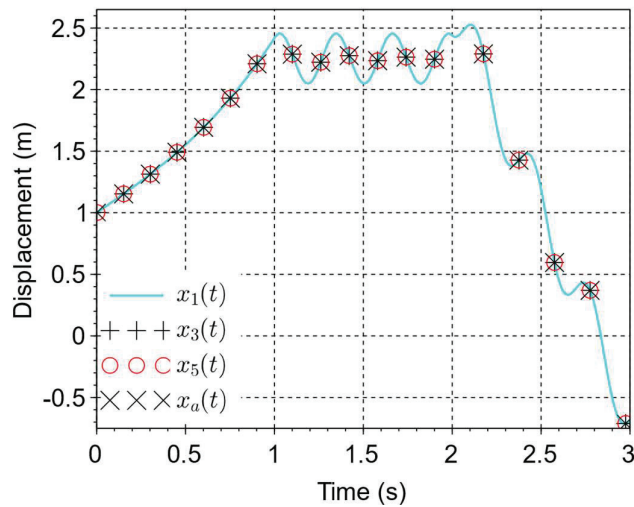


FIGURE 9. Displacements of selected generalized coordinates, incorporating the analytical solution [10].

**3.3. Discussion of this section.** The perpetual points in mathematics defined recently, and herein their application in mechanics and mechanical engineering is discussed. The PMs in linear natural systems are associated with rigid body motions, and this is proved in 2 theorems [7,8].

Further on, based on some new definitions of mechanical systems, and their solutions, the proof of another theorem is straightforward. This theorem defines the conditions that a N-dof flexible mechanical system is moving as a rigid body, and in this case the state space is forming the exact augmented perpetual manifolds. In case of harmonic excitation that leads to a solution in the exact augmented perpetual manifold, the motion of the N-dof mechanical flexible system is a wave particle motion.

The analysis of zero internal forces in the exact augmented perpetual manifolds are in a corollary with proof in [10] and the analysis of the energies in a theorem proved is in an under review article, indicating that flexible dissipative mechanical systems in the exact augmented perpetual manifolds might behave as perpetual machines of 2<sup>nd</sup> and 3<sup>rd</sup> kind. Under review articles, have more corollaries and more theorems under preparation, and combining them might lead to the development of the perpetual mechanics theory.

## 4. Conclusions

In this review article, starting from examining the dynamics of a hybrid system, theorem's development relative to perpetual points applied in mechanics is shown. The dynamic analysis of the hybrid system, a spinning shaft with non-constant rotating speed, through the traditional multiple scales analysis enhanced with a dynamic analysis through linearization around the perpetual points defining the rigid body modes, is performed. Although the nonlinear dynamic analysis formalism is extensive, identifying spinning shaft's critical situations requires further work.

The observation that the perpetual points of the spinning shaft are associated with the rigid body modes, lead to the proof of two theorems, that the pps of linear natural mechanical unforced systems are associated with rigid body modes. Further on some new definitions, such as perpetual mechanical systems, and the augmented perpetual manifolds, lead to the proof of a theorem that defines the conditions for a N-dof flexible mechanical system to move as a rigid body, with state space given by the exact augmented perpetual manifolds. Moreover, if the exact augmented perpetual manifolds arise through harmonic excitation, as a proved corollary states, the N-dof flexible mechanical system moves in dual mode, as wave particle. The last theorem is of high significance in mathematics, mechanics, and mechanical engineering. Since it provides a particular solution of non-autonomous mechanical systems and the system might have dual-mode wave particle motion, which is highly significant in physics. Finally, the rigid body motion without any other vibrations is the ultimate motion in many mechanical engineering applications.

As a continuation of this work, further developments need to identify the spinning shaft's critical situations for non-constant rotating speed, normal modes away from the linearization, and rigid body angular velocities the system's dynamics associated with eigenvalues with positive real part. Moreover the chaotic motions of the spinning shaft needs more work.

There are several directions to be followed for the development of the perpetual mechanics theory e.g. internal energies of the perpetual mechanical systems in the exact augmented perpetual manifolds that lead to perpetual machines behavior, the physics of particle wave motion, properties of the augmented perpetual submanifolds etc., highlighting that many of them are currently in under review articles.

## References

- [1] K.R. (Stevanović) Hedrih, *Linear and nonlinear dynamics of hybrid systems*, Proc. of IMechE: Part-C J. of Mech. Eng. Sci. **235** (20) (2021), 4535-4568. Doi: 10.1177/0954406220957699
- [2] F. Georgiades, *Nonlinear Dynamics of a spinning shaft with non-constant rotating speed*, Nonlinear Dynamics **93** (1) (2018), 89-118.
- [3] F. Georgiades, *Equilibrium points with their associated normal modes describing nonlinear dynamics of a spinning shaft with non-constant rotating speed*, Journal of Vibration Testing and System Dynamics **2** (4) (2018), 327-373.

- [4] F. Georgiades, *Chaotic dynamics in spinning shafts with non-constant rotating speed described by variant Lyapunov exponents*, in: Nonlinear Dynamics of Structures, Systems and Devices, W. Lacarbonara et al (eds.), Proceedings of the First International Nonlinear Dynamics Conference (NODYCON 2019) I, Springer Nature Switzerland AG2020. [https://doi.org/10.1007/978-3-030-34713-0\\_47](https://doi.org/10.1007/978-3-030-34713-0_47)
- [5] A. Prasad, *Existence of perpetual points in nonlinear dynamical systems and its applications*, Int. J. Bif. Chaos **25**(2) (2015), 1530005, Doi: 10.1142/S0218127415300050.
- [6] D. Dudkowski, A. Prasad, T. Kapitaniak, *Perpetual points and hidden attractors in dynamical systems*, Phys. Lett. A **379** (40-41) (2015), 2591-2596.
- [7] F. Georgiades, *Theorem and Observation About the Nature of Perpetual Points in Conservative Mechanical Systems*, In: IUTAM Symposium on Exploiting Nonlinear Dynamics for Engineering Systems, I. Kovacic, S. Lenci, (eds), ENOLIDES 2018, IUTAM Bookseries **37**, Springer Nature Switzerland AG2020. [https://doi.org/10.1007/978-3-030-23692-2\\_9](https://doi.org/10.1007/978-3-030-23692-2_9).
- [8] F. Georgiades, *Perpetual points in natural dissipative with viscous damping mechanical systems: A theorem and a remark*, Proc. of IMechE: Part-C J. of Mech. Eng. Sci, **235** (20) (2021), 4526-4534. Doi: 10.1177/0954406220934833.
- [9] F. Georgiades, *Augmented Perpetual Manifolds and Perpetual Mechanical Systems-Part I: Definitions, Theorem and Corollary for Triggering Perpetual Manifolds, Application in Reduced Order Modeling and Particle-Wave Motion of Flexible Mechanical Systems*, ASME Journal of Computational and Nonlinear Dynamics **16** (7) (2021), 071005. <https://doi.org/10.1115/1.4050554>
- [10] F. Georgiades, *Augmented perpetual manifolds, a corollary: Dynamics of natural mechanical systems with eliminated internal forces*, In: Advances in Nonlinear Dynamics, W. Lacarbonara et al (eds.), NODYCON 2021, NODYCON Conference Proceedings Series, Springer Nature Switzerland AQ 2022 (in press).
- [11] A. Kirk, F. Georgiades, C. Bingham, *Towards Determination of Critical Speeds of a Rotating Shaft with Eccentric Sleeves: Equations of Motion*, Mech. Machine Science, in: Proceedings of 9th IFToMM Int. Conf. on Rotor Dynamics, Mechanisms and Machine Science **21**, P. Pennacchi (ed.), 9<sup>th</sup> IFToMM Int. Conf. on Rotor Dynamics 22-25 September, 2014, Milan, Italy, (2015), 1809-1822, Springer International Publishing Switzerland 2015.
- [12] F. Georgiades, *Corrigendum/Addendum in 'Georgiades, F., 2018, Equilibrium Points with Their Associated Normal Modes Describing Nonlinear Dynamics of a Spinning Shaft with Non-Constant Rotating Speed, Journal of Vibration Testing and System Dynamics, 2(4), 327-373'*, Journal of Vibration Testing and System Dynamics **3** (2) (2019), 231-233.
- [13] A. H. Nayfeh, *A perturbation method for treating nonlinear oscillation problems*. Studies in Applied Mathematics, (1965). Doi: 10.1002/sapm1965441368
- [14] S. Liebscher, *Bifurcation without parameters*, Springer International Publishing Switzerland, 2015. <https://doi.org/10.1007/978-3-319-10777-6>

## Appendix A

### A.1 Solution of torsional with rigid body angular motion, equations.

1<sup>st</sup> order approximation solution of equations (17a-b)

They are obtained in [2,3]:

For  $\Omega^2 < \omega_T$ ,

$$q_{\phi,1}(T_0) = A_{22} \cdot e^{i\mu_0 T_0} + cc, \quad (\text{A.1a})$$

$$\dot{\theta}_1(T_0) = A_{11} + A_{12} \cdot e^{i\mu_0 T_0} + cc, \quad (\text{A.1b})$$

with,

$$\mu_0 = \sqrt{\frac{I_1 \cdot L \cdot (\omega_T^2 - \Omega^2)}{(I_1 \cdot L - F^2)}}, \quad (\text{A.2})$$

and amplitudes given by,

$$A_{22} = \frac{q_{\phi,1}(0)}{2} - i \cdot \frac{\dot{q}_{\phi,1}(0)}{2 \cdot \mu_0} = A_{\phi,1} - i \cdot A_{\phi,2}, \quad (\text{A.3})$$

$$A_{11} = \dot{\theta}_1(0) - \frac{F}{I_1 \cdot L} \cdot \dot{q}_{\phi,1}(0), \quad (\text{A.4a})$$

$$A_{12} = \frac{F}{2 \cdot I_1 \cdot L} \cdot \dot{q}_{\phi,1}(0) + i \cdot \frac{F \cdot \mu_0}{2 \cdot I_1 \cdot L} \cdot q_{\phi,1}(0) = A_{\theta,1} - i \cdot A_{\theta,2}. \quad (\text{A.4b})$$

In case of  $\Omega^2 \geq \omega_T$ , then the eigenvalues are real and given by,

$$\Lambda_5 = \pm \sqrt{\frac{I_1 \cdot L \cdot (\theta_0^2 - \omega_T^2)}{(I_1 \cdot L - F^2)}}, \quad (\text{A.5})$$

and there is no oscillatory motion in torsion, therefore they are not associated with any NNMs or critical situations.

**Amplitudes modulation of 1<sup>st</sup> order approximation.** They are obtained by solving in [2] the equations (18a,b), and they are given :

$$A_{\phi,1}(T_1) = \frac{1}{2} \cdot [A_{\phi,1}(0) + i \cdot A_{\phi,2}(0)] \cdot e^{i\mu_1 T_1} + cc, \quad (\text{A.6a})$$

$$A_{\phi,2}(T_1) = \frac{1}{2} \cdot [A_{\phi,2}(0) - i \cdot A_{\phi,1}(0)] \cdot e^{i\mu_1 T_1} + cc, \quad (\text{A.6b})$$

$$A_{\theta,1}(T_1) = \frac{1}{2} \cdot [A_{\theta,1}(0) + i \cdot A_{\theta,2}(0)] \cdot e^{i\mu_1 T_1} + cc, \quad (\text{A.6c})$$

$$A_{\theta,2}(T_1) = \frac{1}{2} \cdot [A_{\theta,2}(0) - i \cdot A_{\theta,1}(0)] \cdot e^{i\mu_1 T_1} + cc, \quad (\text{A.6d})$$

with,

$$\mu_1 = \frac{I_1 \cdot L \cdot \Omega \cdot A_{11}}{\mu_0 \cdot (I_1 \cdot L - F^2)}, \quad (\text{A.7})$$

and in case of  $\mu_0$  equal to zero equation (A.7) becomes singular.

Lead to the following 1st order approximation solution,

$$q_{\phi,1}(T_0, T_1) = A_{22}(0) \cdot e^{i(\mu_0 T_0 - \varepsilon \cdot \mu_1 \cdot T_1)} + cc, \quad (\text{A.8a})$$

$$\dot{\theta}_1(T_0, T_1) = \frac{A_{11}}{2} + A_{12}(0) \cdot e^{i(\mu_0 T_0 - \varepsilon \cdot \mu_1 \cdot T_1)} + cc. \quad (\text{A.8b})$$

**2<sup>nd</sup> order approximation solution of equations (19a-b)**

It is given by [2]:

$$q_{\phi,2}(T_0) = R_{2,0}(T_1) \cdot e^{i\mu_0 T_0} + R_{2,1}(T_1) \cdot e^{i2\mu_0 T_0} + R_{2,2}(T_1) \cdot e^{i2\omega_1 T_0} + \\ + R_{2,3}(T_1) \cdot e^{i2\omega_2 T_0} + R_{2,4}(T_1) \cdot e^{i(\omega_1+\omega_2)T_0} + R_{2,5}(T_1) \cdot e^{i(\omega_1-\omega_2)T_0} + cc, \quad (\text{A.9})$$

with,

$$R_{2,0}(T_1) = \frac{1}{6\mu_0^2} [3 \cdot V_1(T_1) - \bar{V}_1(T_1)] + \\ + \frac{V_2(T_1) \cdot (2\omega_1 + \mu_0) - \bar{V}_2(T_1) \cdot (2\omega_1 - \mu_0)}{2\mu_0 \cdot (4\omega_1^2 - \mu_0^2)} + \\ + \frac{V_3(T_1) \cdot (2\omega_2 + \mu_0) - \bar{V}_3(T_1) \cdot (2\omega_2 - \mu_0)}{2\mu_0 \cdot (4\omega_2^2 - \mu_0^2)} + \frac{V_4(T_1) \cdot (\omega_1 + \omega_2 + \mu_0)}{2\mu_0 \cdot [(\omega_1 + \omega_2)^2 - \mu_0^2]} + \\ - \frac{\bar{V}_4(T_1) \cdot (\omega_1 + \omega_2 - \mu_0)}{2\mu_0 \cdot [(\omega_1 + \omega_2)^2 - \mu_0^2]} + \frac{V_5(T_1) \cdot (\omega_1 - \omega_2 + \mu_0) - \bar{V}_5(T_1) \cdot (\omega_1 - \omega_2 - \mu_0)}{2\mu_0 \cdot [(\omega_1 - \omega_2)^2 - \mu_0^2]}, \quad (\text{A.10a})$$

$$R_{2,1}(T_1) = -\frac{V_1(T_1)}{3\mu_0^2}, \quad (\text{A.10b})$$

$$R_{2,2}(T_1) = -\frac{V_2(T_1)}{(4\omega_1^2 - \mu_0^2)}, \quad (\text{A.10c})$$

$$R_{2,3}(T_1) = -\frac{V_3(T_1)}{(4\omega_2^2 - \mu_0^2)}, \quad (\text{A.10d})$$

$$R_{2,4}(T_1) = -\frac{V_4(T_1)}{[(\omega_1 + \omega_2)^2 - \mu_0^2]}, \quad (\text{A.10e})$$

$$R_{2,5}(T_1) = -\frac{V_5(T_1)}{[(\omega_1 - \omega_2)^2 - \mu_0^2]}. \quad (\text{A.10f})$$

and,

$$\dot{\theta}_2(T_0) = U_{2,0}(T_1) + U_{2,1}(T_1)e^{i\mu_0 T_0} + U_{2,2}(T_1) \cdot e^{i2\mu_0 T_0} + U_{2,3}(T_1) \cdot e^{i2\omega_1 T_0} + \\ + U_{2,4}(T_1) \cdot e^{i2\omega_2 T_0} + U_{2,5}(T_1) \cdot e^{i(\omega_1+\omega_2)T_0} + U_{2,6}(T_1) \cdot e^{i(\omega_1-\omega_2)T_0} + cc, \quad (\text{A.11})$$

with,

$$U_{2,1}(T_1) = -\frac{i \cdot S_0 \cdot R_{2,0}(T_1)}{\mu_0}, \quad (\text{A.12a})$$

$$U_{2,2}(T_1) = -\frac{i \cdot [S_0 \cdot R_{2,1}(T_1) + S_1(T_1)]}{2\mu_0}, \quad (\text{A.12b})$$

$$U_{2,3}(T_1) = -\frac{i \cdot [S_0 \cdot R_{2,2}(T_1) + S_2(T_1)]}{2\omega_1}, \quad (\text{A.12c})$$

$$U_{2,4}(T_1) = -\frac{i \cdot [S_0 \cdot R_{2,3}(T_1) + S_3(T_1)]}{2\omega_2}, \quad (\text{A.12d})$$

$$U_{2,5}(T_1) = -\frac{i \cdot [S_0 \cdot R_{2,4}(T_1) + S_4(T_1)]}{(\omega_1 + \omega_2)}, \quad (\text{A.12e})$$

$$U_{2,6}(T_1) = -\frac{i \cdot [S_0 \cdot R_{2,5}(T_1) + S_5(T_1)]}{(\omega_1 - \omega_2)}, \quad (\text{A.12f})$$

$$U_{2,0}(T_1) = -\sum_{j=1}^6 U_{2,j}(T_1). \quad (\text{A.12g})$$

## A.2 Solution of lateral bending motion equations.

### 1<sup>st</sup> order approximation solution, of equations (22a-b)

The eigenvalues that lead to natural frequencies are depended in the following two parameters [2]:

$$\eta_1 = -\omega_b^2 - \frac{(M+1)}{(1-M)^2} \cdot \Omega^2, \quad (\text{A.13a})$$

and,

$$\eta_2 = \frac{4 \cdot \Omega^2}{(1-M)^2} \cdot \left( \frac{M \cdot \Omega^2}{(1-M)^2} + \omega_b^2 \right), \quad (\text{A.13b})$$

The first parameter ( $\eta_1$ ) is negative for,

$$\frac{L^2}{(r_0^2 + r_1^2)} > \frac{\pi^2}{4} \cong 2.5 \Leftrightarrow L^2 > 2.5 \cdot (r_0^2 + r_1^2). \quad (\text{A.14a})$$

Rule of thumb for Euler-Bernoulli solid beams is,

$$\frac{L}{r_0} > 10 \Rightarrow L^2 > 100 \cdot r_0^2 > 2.5 \cdot r_0^2, \quad (\text{A.14b})$$

therefore, for all solid Euler-Bernoulli beams  $\eta_1 < 0$ .

In case of hollow beams a practical consideration could be,

$$\frac{L^2}{(r_0^2 + r_1^2)} > \frac{L^2}{2 \cdot r_0^2} > \frac{\pi^2}{4} \Rightarrow L > 2.22 \cdot r_0. \quad (\text{A.14c})$$

In conclusion, the parameter  $\eta_1$  is negative for sufficient small dimension of the cross section with respect to the shaft length that applies in many Euler Bernoulli shaft configurations.

Considering positive angular velocity, the 2<sup>nd</sup> parameter ( $\eta_2$ ) is positive as long as,

$$\begin{aligned} \eta_2 > 0 &\Leftrightarrow \frac{M \cdot \Omega^2}{(1-M)^2} + \omega_b^2 > 0 \Leftrightarrow -|M| \cdot \Omega^2 + (1-M)^2 \cdot \omega_b^2 > 0 \Leftrightarrow \\ &\Leftrightarrow |M| \cdot \Omega^2 < (1-M)^2 \cdot \omega_b^2 \Leftrightarrow \Omega^2 < \frac{(1-M)^2 \cdot \omega_b^2}{|M|} \Rightarrow \Omega < \frac{(1-M) \cdot \omega_b}{\sqrt{-M}}. \end{aligned} \quad (\text{A.14d})$$

The eigenvalues are given by,

$$\lambda = \pm \sqrt{\eta_1 \pm \sqrt{\eta_2}}. \quad (\text{A.15})$$

Considering equations (A.13a,b) in equation (A.15) then the following three cases for the definitions of the eigenvalues might happen [2],

Case 1  $\eta_2 > 0$ ,  $\eta_1 + \sqrt{\eta_2} < 0$ .

Case 2  $\eta_2 > 0$ ,  $\eta_1 + \sqrt{\eta_2} > 0$ .

Case 3  $\eta_2 < 0$ .

In [3] different definitions of parameters are used and makes profound that the 2<sup>nd</sup> case can never exist, as follows,

$$\eta_1 = \frac{-(a_3^2 - 2 \cdot a_1)}{2}, \quad (\text{A.16a})$$

$$\eta_2 = \frac{(a_3^2 - 2 \cdot a_1)^2 - 4 \cdot a_1^2}{4}, \quad (\text{A.16b})$$

which lead to,

$$\eta_1 + \sqrt{\eta_2} = \frac{-(a_3^2 - 2 \cdot a_1)}{2} + \sqrt{\frac{(a_3^2 - 2 \cdot a_1)^2 - 4 \cdot a_1^2}{4}} < 0, \quad (\text{A.16c})$$

whereas the parameters  $a_1$  and  $a_3$  by equations (46b) and (46d) respectively are defined (using the consistent notation of  $\Omega = \dot{\theta}_0$ ).

Summarizing the eigenvalue analysis of [2] and [3], then, only the 1<sup>st</sup> and 3<sup>rd</sup> case exist as follows:

Case I,  $\eta_2 \geq 0$ , then the eigenvalues are purely imaginary and they are given by,

$$\lambda_{2,1} = -i \sqrt{-\eta_1 - \sqrt{\eta_2}} = -i\omega_1, \quad (\text{A.17a})$$

$$\lambda_{2,2} = -i \sqrt{-\eta_1 + \sqrt{\eta_2}} = -i\omega_2, \quad (\text{A.17b})$$

$$\lambda_{2,3} = i \sqrt{-\eta_1 - \sqrt{\eta_2}} = i\omega_1, \quad (\text{A.17c})$$

$$\lambda_{2,4} = i \sqrt{-\eta_1 + \sqrt{\eta_2}} = i\omega_2, \quad (\text{A.17d})$$

with natural frequencies given by,

$$\omega_{1 \div 2} = 2 \cdot \pi \cdot f_{1 \div 2} = \sqrt{\omega_b^2 + \frac{(M+1)}{(1-M)^2} \cdot \Omega^2 \mp \frac{2 \cdot \Omega}{(1-M)} \cdot \sqrt{\frac{M \cdot \Omega^2}{(1-M)^2} + \omega_b^2}}. \quad (\text{A.18a-b})$$

and this is true for rigid body angular velocities that obey inequality (A.14d).

Case II,  $\eta_2 \geq 0$ , then the eigenvalues are not purely imaginary any longer and they are given by [3],

$$\lambda_{4 \div 7}(\dot{\theta}_0) = \pm \left( \sqrt{\frac{-M\Omega^2}{(1-M)^2} - \omega_b^2} \pm i \frac{\Omega}{(1-M)} \right) = \pm (\Lambda_6 \pm i\Lambda_7), \quad (\text{A.19a-d})$$

and this is true as long as the rigid body angular velocities do not obey inequality (A.13d).

Further on, for pure imaginary eigenvalues (case I) the solutions are given by,

$$q_{v,1}(T_0) = C_{v1} \cdot e^{i\omega_1 T_0} + D_{v1} \cdot e^{i\omega_2 T_0} + cc, \quad (\text{A.20a})$$

$$q_{w,1}(T_0) = C_{w1} \cdot e^{i\omega_1 T_0} + D_{w1} \cdot e^{i\omega_2 T_0} + cc, \quad (\text{A.20b})$$

$$\dot{q}_{v,1}(T_0) = i \cdot \omega_1 \cdot C_{v1} \cdot e^{i\omega_1 T_0} + i \cdot \omega_2 \cdot D_{v1} \cdot e^{i\omega_2 T_0} + cc, \quad (\text{A.20c})$$

$$\dot{q}_{w,1}(T_0) = i \cdot \omega_1 \cdot C_{w1} \cdot e^{i\omega_1 T_0} + i \cdot \omega_2 \cdot D_{w1} \cdot e^{i\omega_2 T_0} + cc, \quad (\text{A.20d})$$

With,

$$C_{v1} = -d_{n2} \cdot \dot{q}_{w,1}(0) - d_{n2} \cdot d_2 \cdot q_{v,1}(0) + i \cdot (d_{n1} \cdot \omega_1 \cdot d_2 \cdot \dot{q}_{v,1}(0) - d_{n1} \cdot \omega_1 \cdot \omega_2^2 \cdot q_{w,1}(0)) = B_{v1,1} + i \cdot B_{v2,1}, \quad (\text{A.21a})$$

$$D_{v1} = d_{n2} \cdot \dot{q}_{w,1}(0) + d_{n2} \cdot b_2 \cdot q_{v,1}(0) + i \cdot (-d_{n1} \cdot b_2 \cdot \omega_2 \cdot \dot{q}_{v,1}(0) + d_{n1} \cdot \omega_1^2 \cdot \omega_2 \cdot q_{w,1}(0)) = B_{v1,2} + i \cdot B_{v2,2}, \quad (\text{A.21b}), \quad (\text{A.21b})$$

$$C_{w1} = -d_{n1} \cdot b_2 \cdot d_2 \cdot \dot{q}_{v,1}(0) + d_{n1} \cdot b_2 \cdot \omega_2^2 \cdot q_{w,1}(0) + i \cdot \left[ -d_{n2} \cdot \left( \frac{b_2}{\omega_1} \right) \cdot \dot{q}_{w,1}(0) - d_{n2} \cdot \left( \frac{b_2 \cdot d_2}{\omega_1} \right) \cdot q_{v,1}(0) \right] = B_{w1,1} + i \cdot B_{w2,1}, \quad (\text{A.21c})$$

$$D_{w1} = d_{n1} \cdot b_2 \cdot d_2 \cdot \dot{q}_{v,1}(0) - d_{n1} \cdot \omega_1^2 \cdot d_2 \cdot q_{w,1}(0) + \\ + i \cdot \left[ d_{n2} \cdot \left( \frac{d_2}{\omega_2} \right) \cdot \dot{q}_{w,1}(0) + d_{n2} \cdot \left( \frac{b_2 d_2}{\omega_2} \right) \cdot q_{v,1}(0) \right] = B_{w1,2} + i \cdot B_{w2,2}, \quad (\text{A.21d})$$

$$b_2 = \frac{-\Omega^2 + (1-M) \cdot (\omega_b^2 - \omega_1^2)}{2 \cdot \Omega}, \quad (\text{A.22a})$$

$$d_2 = \frac{-\Omega^2 + (1-M) \cdot (\omega_b^2 - \omega_2^2)}{2 \cdot \Omega}, \quad (\text{A.22b})$$

$$d_{n1} = \frac{\Omega}{[-\Omega^2 + (1-M) \cdot (\omega_b^2 - \omega_1^2)] \cdot \omega_2^2 - [-\Omega^2 + (1-M) \cdot (\omega_b^2 - \omega_2^2)] \cdot \omega_1^2}, \quad (\text{A.22c})$$

$$d_{n2} = \frac{\Omega}{(1-M) \cdot (\omega_2^2 - \omega_1^2)}. \quad (\text{A.22d})$$

Amplitudes modulation of 1<sup>st</sup> order approximation, determined by the solution of the systems of equations (23)

The eigenvalues of this system are given by [2],

$$\lambda_{4,j,1} = -A_{11} \cdot \left( \frac{\Omega - \omega_j}{(1-M) \cdot \omega_j - \Omega} \right) \cdot i = \omega_{det,j,1} \cdot i, \quad (\text{A.23a})$$

$$\lambda_{4,j,2} = -A_{11} \cdot \left( \frac{\Omega + \omega_j}{(1-M) \cdot \omega_j + \Omega} \right) \cdot i = -\omega_{det,j,2} \cdot i, \quad (\text{A.23b})$$

$$\lambda_{4,j,3} = -\omega_{det,j,1} \cdot i, \quad (\text{A.23c})$$

$$\lambda_{4,j,4} = \omega_{det,j,2} \cdot i. \quad (\text{A.23d})$$

whereas,  $j=1$  corresponds to the system arising from first frequency ( $\omega_1$ ) and  $j=2$  to the system arising from the second frequency ( $\omega_2$ ).

Then, the solution of the system eq. (23) is given by,

$$B_{v1,j}(T_1) = (Q_{R1,j} + i \cdot Q_{I1,j}) \cdot e^{i \cdot \omega_{det,j,1} \cdot T_1} + (Q_{R2,j} + i \cdot Q_{I2,j}) \cdot e^{i \cdot \omega_{det,j,2} \cdot T_1} + cc, \quad (\text{A.24a})$$

$$B_{v2,j}(T_1) = (P_{R1,j} + i \cdot P_{I1,j}) \cdot e^{i \cdot \omega_{det,j,1} \cdot T_1} + (P_{R2,j} + i \cdot P_{I2,j}) \cdot e^{i \cdot \omega_{det,j,2} \cdot T_1} + cc, \quad (\text{A.24b})$$

$$B_{w1,j}(T_1) = (U_{R1,j} + i \cdot U_{I1,j}) \cdot e^{i \cdot \omega_{det,j,1} \cdot T_1} + (U_{R2,j} + i \cdot U_{I2,j}) \cdot e^{i \cdot \omega_{det,j,2} \cdot T_1} + cc, \quad (\text{A.24c})$$

$$B_{w2,j}(T_1) = (S_{R1,j} + i \cdot S_{I1,j}) \cdot e^{i \cdot \omega_{det,j,1} \cdot T_1} + (S_{R2,j} + i \cdot S_{I2,j}) \cdot e^{i \cdot \omega_{det,j,2} \cdot T_1} + cc, \quad (\text{A.24d})$$

with amplitudes for:

$B_{v1,j}(T_1)$  given by,

$$Q_{R1,j} = f_{j,1} \cdot p_{j,1} \cdot B_{v1,j}(0) - g_{j,1} \cdot p_{j,1} \cdot B_{w2,j}(0), \quad (\text{A.25a})$$

$$Q_{I1,j} = e_{j,1} \cdot p_{j,1} \cdot B_{v2,j}(0) - h_{j,1} \cdot p_{j,1} \cdot B_{w1,j}(0), \quad (\text{A.25b})$$

$$Q_{R2,j} = -f_{j,2} \cdot p_{j,2} \cdot B_{v1,j}(0) + g_{j,2} \cdot p_{j,2} \cdot B_{w2,j}(0), \quad (\text{A.25c})$$

$$Q_{I2,j} = e_{j,2} \cdot p_{j,2} \cdot B_{v2,j}(0) + h_{j,1} \cdot p_{j,2} \cdot B_{w1,j}(0), \quad (\text{A.25d})$$

$B_{v2,j}(T_1)$  given by,

$$P_{R1,j} = e_{j,1} \cdot B_{v2,j}(0) - h_{j,1} \cdot B_{w1,j}(0), \quad (\text{A.25e})$$

$$P_{I1,j} = -f_{j,1} \cdot B_{v1,j}(0) + g_{j,1} \cdot B_{w2,j}(0), \quad (\text{A.25f})$$

$$P_{R2,j} = e_{j,2} \cdot B_{v2,j}(0) + h_{j,1} \cdot B_{w1,j}(0), \quad (\text{A.25g})$$

$$P_{I2,j} = f_{j,2} \cdot B_{v1,j}(0) - g_{j,2} \cdot B_{w2,j}(0), \quad (\text{A.25h})$$

$B_{w1,j}(T_1)$  given by,

$$U_{R1,j} = e_{j,1} \cdot r_{j,1} \cdot B_{v2,j}(0) - h_{j,1} \cdot r_{j,1} \cdot B_{w1,j}(0), \quad (\text{A.25i})$$

$$U_{I1,j} = -f_{j,1} \cdot r_{j,1} \cdot B_{v1,j}(0) + g_{j,1} \cdot r_{j,1} \cdot B_{w2,j}(0), \quad (\text{A.25j})$$

$$U_{R2,j} = e_{j,2} \cdot r_{j,2} \cdot B_{v2,j}(0) + h_{j,1} \cdot r_{j,2} \cdot B_{w1,j}(0), \quad (\text{A.25k})$$

$$U_{I2,j} = f_{j,2} \cdot r_{j,2} \cdot B_{v1,j}(0) - g_{j,2} \cdot r_{j,2} \cdot B_{w2,j}(0), \quad (\text{A.25l})$$

$B_{w2,j}(T_1)$  given by,

$$S_{R1,j} = f_{j,1} \cdot q_{j,1} \cdot B_{v1,j}(0) - g_{j,1} \cdot q_{j,1} \cdot B_{w2,j}(0), \quad (\text{A.25m})$$

$$S_{I1,j} = e_{j,1} \cdot q_{j,1} \cdot B_{v2,j}(0) - h_{j,1} \cdot q_{j,1} \cdot B_{w1,j}(0), \quad (\text{A.25n})$$

$$S_{R2,j} = -f_{j,2} \cdot q_{j,2} \cdot B_{v1,j}(0) + g_{j,2} \cdot q_{j,2} \cdot B_{w2,j}(0), \quad (\text{A.25o})$$

$$S_{I2,j} = e_{j,2} \cdot q_{j,2} \cdot B_{v2,j}(0) + h_{j,1} \cdot q_{j,2} \cdot B_{w1,j}(0). \quad (\text{A.25p})$$

And the parameters are given by,

$$p_{j,k} = \frac{j_{j,k}}{d_{j,k} \cdot \omega_{det,j,k}}, \quad (\text{A.26a})$$

$$q_{j,k} = \frac{k_{j,k}}{d_{j,k} \cdot \omega_{det,j,k}}, \quad (\text{A.26b})$$

$$r_{j,k} = \frac{l_{j,k}}{d_{j,k} \cdot l_{j,2}}, \text{ with } k=1,2, \quad (\text{A.26c})$$

$$e_{j,1} = \frac{d_{j,k} \cdot l_{j,2}}{m_{j,1}}, \quad (\text{A.26d})$$

$$e_{j,2} = \frac{-d_{j,2} \cdot l_{j,1}}{m_{j,1}}, \quad (\text{A.26e})$$

$$f_{j,1} = \frac{d_{j,1} \cdot k_{j,2} \cdot \omega_{det,j,1}}{m_{j,2}}, \quad (\text{A.26f})$$

$$f_{j,2} = \frac{d_{j,2} \cdot k_{j,1} \cdot \omega_{det,j,2}}{m_{j,2}}, \quad (\text{A.26g})$$

$$g_{j,1} = \frac{d_{j,1} \cdot j_{j,2} \cdot \omega_{det,j,1}}{m_{j,2}}, \quad (\text{A.26h})$$

$$g_{j,2} = \frac{d_{j,2} \cdot j_{j,1} \cdot \omega_{det,j,2}}{m_{j,2}}, \quad (\text{A.26i})$$

$$h_{j,1} = \frac{d_{j,1} \cdot d_{j,2}}{m_{j,1}}, \quad (\text{A.26j})$$

$$d_{j,k} = a_{3,j}^2 \cdot \omega_{det,j,k}^2 \cdot \Omega - 2 \cdot a_{3,j} \cdot b_3 \cdot c_{3,j} + b_3^2 \cdot \Omega + c_{3,j}^2 \cdot \Omega - \omega_{det,j,k}^2 \cdot \Omega^3, \quad (\text{A.26k})$$

$$j_{j,k} = a_{3,j}^2 \cdot c_{3,j} \cdot \omega_{det,j,k}^2 - 2 \cdot a_{3,j} \cdot b_3 \cdot \omega_{det,j,k}^2 \cdot \Omega + b_3^2 \cdot c_{3,j} - c_{3,j}^3 + c_{3,j} \cdot \omega_{det,j,k}^2 \cdot \Omega^2, \quad (\text{A.26l})$$

$$k_{j,k} = a_{3,j}^2 \cdot b_3 \cdot \omega_{det,j,k}^2 - 2 \cdot a_{3,j} \cdot c_{3,j} \cdot \omega_{det,j,k}^2 \cdot \Omega + b_3 \cdot c_{3,j}^2 - b_3^3 + b_3 \cdot \omega_{det,j,k}^2 \cdot \Omega^2, \quad (\text{A.26m})$$

$$l_{j,k} = a_{3,j}^3 \cdot \omega_{det,j,k}^2 - a_{3,j} \cdot b_3^2 - a_{3,j} \cdot c_{3,j}^2 - a_{3,j} \cdot \omega_{det,j,k}^2 \cdot \Omega^2 + 2 \cdot b_3 \cdot c_{3,j} \cdot \Omega, \quad (\text{A.26n})$$

$$m_{j,1} = 2 \cdot (d_{j,1} \cdot l_{j,2} - d_{j,2} \cdot l_{j,1}), \quad (\text{A.26o})$$

$$m_{j,2} = 2 \cdot (j_{j,1} \cdot k_{j,2} - j_{j,2} \cdot k_{j,1}) . \quad (\text{A.26p})$$

Combining both scales solutions lead to [2],

$$\begin{aligned} q_{v,1}(T_0, T_1) = & 2 \cdot \sum_{j=1}^2 \sum_{k=1}^2 [(Q_{Rj,k} - P_{Ij,k}) \cdot \cos(\omega_k \cdot T_0 + \varepsilon \cdot \omega_{det,k,j} \cdot T_1)] - \\ & - 2 \cdot \sum_{j=1}^2 \sum_{k=1}^2 [(Q_{Ij,k} + P_{Rj,k}) \cdot \sin(\omega_k \cdot T_0 + \varepsilon \cdot \omega_{det,k,j} \cdot T_1)] + \\ & + 2 \cdot \sum_{j=1}^2 \sum_{k=1}^2 [(Q_{Rj,k} + P_{Ij,k}) \cdot \cos(\omega_k \cdot T_0 - \varepsilon \cdot \omega_{det,k,j} \cdot T_1)] - \\ & - 2 \cdot \sum_{j=1}^2 \sum_{k=1}^2 [(P_{Rj,k} - Q_{Ij,k}) \cdot \sin(\omega_k \cdot T_0 - \varepsilon \cdot \omega_{det,k,j} \cdot T_1)] , \end{aligned} \quad (\text{A.27a})$$

$$\begin{aligned} q_{w,1}(T_0, T_1) = & 2 \cdot \sum_{j=1}^2 \sum_{k=1}^2 [(U_{Rj,k} - S_{Ij,k}) \cdot \cos(\omega_k \cdot T_0 + \varepsilon \cdot \omega_{det,k,j} \cdot T_1)] - \\ & - 2 \cdot \sum_{j=1}^2 \sum_{k=1}^2 [(U_{Ij,k} + S_{Rj,k}) \cdot \sin(\omega_k \cdot T_0 + \varepsilon \cdot \omega_{det,k,j} \cdot T_1)] + \\ & + 2 \cdot \sum_{j=1}^2 \sum_{k=1}^2 [(U_{Rj,k} + S_{Ij,k}) \cdot \cos(\omega_k \cdot T_0 - \varepsilon \cdot \omega_{det,k,j} \cdot T_1)] - \\ & - 2 \cdot \sum_{j=1}^2 \sum_{k=1}^2 [(S_{Rj,k} - U_{Ij,k}) \cdot \sin(\omega_k \cdot T_0 - \varepsilon \cdot \omega_{det,k,j} \cdot T_1)] , \end{aligned} \quad (\text{A.27b})$$

## 2<sup>nd</sup> order approximation solution, of equations (25a-b)

They are obtained in [2], and given by:

$$\begin{aligned} q_{v,2}(T_0, T_1) = & W_{2,1,3}(T_1) \cdot e^{i \cdot \omega_1 \cdot T_0} + W_{2,2,3}(T_1) \cdot e^{i \cdot \omega_2 \cdot T_0} + W_{2,3,3}(T_1) \cdot e^{i \cdot (\mu_0 + \omega_1) \cdot T_0} + \\ & + W_{2,4,3}(T_1) \cdot e^{i \cdot (\mu_0 + \omega_2) \cdot T_0} + W_{2,5,3}(T_1) \cdot e^{i \cdot (\mu_0 - \omega_1) \cdot T_0} + W_{2,6,3}(T_1) \cdot e^{i \cdot (\mu_0 - \omega_2) \cdot T_0} + cc, \quad (\text{A.28a}) \\ q_{w,2}(T_0, T_1) = & W_{2,1,4}(T_1) \cdot e^{i \cdot \omega_1 \cdot T_0} + W_{2,2,4}(T_1) \cdot e^{i \cdot \omega_2 \cdot T_0} + W_{2,3,4}(T_1) \cdot e^{i \cdot (\mu_0 + \omega_1) \cdot T_0} + \\ & + W_{2,4,4}(T_1) \cdot e^{i \cdot (\mu_0 + \omega_2) \cdot T_0} + W_{2,5,4}(T_1) \cdot e^{i \cdot (\mu_0 - \omega_1) \cdot T_0} + W_{2,6,4}(T_1) \cdot e^{i \cdot (\mu_0 - \omega_2) \cdot T_0} + cc, \quad (\text{A.28b}) \end{aligned}$$

with,

$$\begin{aligned} W_{2,1,j}(T_1) = & \sum_{k=1}^2 \left[ \frac{[{}^i F_{k+1,1}(T_1) \cdot C_{j,k,a}(\mu_0 + 2 \cdot \omega_1) - i \cdot \bar{F}_{k+1,1}(T_1) \cdot C_{j,k,a} \mu_0]}{(\mu_0 + \omega_1)^2 - \omega_1^2} \right] +, \\ & + \sum_{k=1}^2 \left[ \frac{[{}^i F_{k+1,2}(T_1) \cdot C_{j,k,a}(\mu_0 + \omega_1 + \omega_2) - i \cdot \bar{F}_{k+1,2}(T_1) \cdot C_{j,k,a}(\mu_0 - \omega_1 + \omega_2)]}{(\mu_0 + \omega_2)^2 - \omega_1^2} \right] +, \\ & + \sum_{k=1}^2 \left[ \frac{[{}^i F_{k+1,3}(T_1) \cdot C_{j,k,a} \mu_0 - i \cdot \bar{F}_{k+1,3}(T_1) \cdot C_{j,k,a}(\mu_0 - 2 \cdot \omega_1)]}{(\mu_0 - \omega_1)^2 - \omega_1^2} \right] +, \\ & + \sum_{k=1}^2 \left[ \frac{[{}^i F_{k+1,4}(T_1) \cdot C_{j,k,a}(\mu_0 + \omega_1 - \omega_2) - i \cdot \bar{F}_{k+1,4}(T_1) \cdot C_{j,k,a}(\mu_0 - \omega_1 - \omega_2)]}{(\mu_0 - \omega_2)^2 - \omega_1^2} \right], \text{with } j=3:4, \end{aligned} \quad (\text{A.29a})$$

$$\begin{aligned} W_{2,2,j}(T_1) = & \sum_{k=1}^2 \left[ \frac{[{}^i F_{k+1,1}(T_1) \cdot C_{j,k,b}(\mu_0 + \omega_1 + \omega_2) - i \cdot \bar{F}_{k+1,1}(T_1) \cdot C_{j,k,b}(\mu_0 + \omega_1 - \omega_2)]}{(\mu_0 + \omega_1)^2 - \omega_2^2} \right] +, \\ & + \sum_{k=1}^2 \left[ \frac{[{}^i F_{k+1,2}(T_1) \cdot C_{j,k,b}(\mu_0 + 2 \cdot \omega_2) - i \cdot \bar{F}_{k+1,2}(T_1) \cdot C_{j,k,b} \mu_0]}{(\mu_0 + \omega_2)^2 - \omega_2^2} \right] +, \\ & + \sum_{k=1}^2 \left[ \frac{[{}^i F_{k+1,3}(T_1) \cdot C_{j,k,b}(\mu_0 - \omega_1 + \omega_2) - i \cdot \bar{F}_{k+1,3}(T_1) \cdot C_{j,k,b}(\mu_0 - \omega_1 - \omega_2)]}{(\mu_0 - \omega_1)^2 - \omega_2^2} \right] +, \\ & + \sum_{k=1}^2 \left[ \frac{[{}^i F_{k+1,4}(T_1) \cdot C_{j,k,b} \mu_0 - i \cdot \bar{F}_{k+1,4}(T_1) \cdot C_{j,k,b}(\mu_0 - 2 \cdot \omega_2)]}{(\mu_0 - \omega_2)^2 - \omega_2^2} \right], \text{with } j=3:4, \end{aligned} \quad (\text{A.29b})$$

$$\begin{aligned} W_{2,3,j}(T_1) = & - \sum_{k=1}^2 \left[ \frac{[{}^i F_{k+1,1}(T_1) \cdot C_{j,k,a}(\mu_0 + 2 \cdot \omega_1) + i \cdot \bar{F}_{k+1,1}(T_1) \cdot \bar{C}_{j,k,a} \mu_0]}{(\mu_0 + \omega_1)^2 - \omega_1^2} \right] -, \\ & - \sum_{k=1}^2 \left[ \frac{[{}^i F_{k+1,1}(T_1) \cdot C_{j,k,b}(\mu_0 + \omega_1 + \omega_2) + i \cdot \bar{F}_{k+1,1}(T_1) \cdot \bar{C}_{j,k,b}(\mu_0 + \omega_1 - \omega_2)]}{(\mu_0 + \omega_1)^2 - \omega_2^2} \right], \text{with } j=3:4, \end{aligned} \quad (\text{A.29c})$$

$$\begin{aligned}
& W_{2,4,j}(T_1) = \\
& = -\sum_{k=1}^2 \left[ \frac{i \cdot F_{k+1,2}(T_1) \cdot C_{j,k,a}(\mu_0 + \omega_1 + \omega_2) + i \cdot F_{k+1,2}(T_1) \cdot \bar{C}_{j,k,a}(\mu_0 - \omega_1 + \omega_2)}{(\mu_0 + \omega_2)^2 - \omega_1^2} \right] - , \\
& - \sum_{k=1}^2 \left[ \frac{i \cdot F_{k+1,2}(T_1) \cdot C_{j,k,b}(\mu_0 + 2 \cdot \omega_2) + i \cdot F_{k+1,2}(T_1) \cdot \bar{C}_{j,k,b} \mu_0}{(\mu_0 + \omega_2)^2 - \omega_2^2} \right], \text{ with } j=3:4 \quad (\text{A.29d})
\end{aligned}$$

$$\begin{aligned}
& W_{2,5,j}(T_1) = -\sum_{k=1}^2 \left[ \frac{i \cdot F_{k+1,3}(T_1) \cdot C_{j,k,a} \mu_0 + i \cdot F_{k+1,3}(T_1) \cdot \bar{C}_{j,k,a}(\mu_0 - 2 \cdot \omega_1)}{(\mu_0 - \omega_1)^2 - \omega_1^2} \right] - , \\
& - \sum_{k=1}^2 \left[ \frac{i \cdot F_{k+1,3}(T_1) \cdot C_{j,k,b}(\mu_0 - \omega_1 + \omega_2) + i \cdot F_{k+1,3}(T_1) \cdot \bar{C}_{j,k,b}(\mu_0 - \omega_1 - \omega_2)}{(\mu_0 - \omega_1)^2 - \omega_2^2} \right], \text{ with } j=3:4, \quad (\text{A.29e})
\end{aligned}$$

$$\begin{aligned}
& W_{2,6,j}(T_1) = -\sum_{k=1}^2 \left[ \frac{i \cdot F_{k+1,4}(T_1) \cdot C_{j,k,a}(\mu_0 + \omega_1 - \omega_2) + i \cdot F_{k+1,4}(T_1) \cdot \bar{C}_{j,k,a}(\mu_0 - \omega_1 - \omega_2)}{(\mu_0 - \omega_2)^2 - \omega_1^2} \right] - , \\
& - \sum_{k=1}^2 \left[ \frac{i \cdot F_{k+1,4}(T_1) \cdot C_{j,k,b} \mu_0 + i \cdot F_{k+1,4}(T_1) \cdot \bar{C}_{j,k,b}(\mu_0 - 2 \cdot \omega_2)}{(\mu_0 - \omega_2)^2 - \omega_2^2} \right], \text{ with } j=3:4, \quad (\text{A.29f})
\end{aligned}$$

and their parameters are given by,

$$C_{3,1,a} = i \cdot \omega_1 \cdot d_2 \cdot d_{n1}, \quad (\text{A.30a})$$

$$C_{3,1,b} = -i \cdot \omega_2 \cdot b_2 \cdot d_{n1}, \quad (\text{A.30b})$$

$$C_{3,2,a} = -d_{n2}, \quad (\text{A.30c})$$

$$C_{3,2,b} = d_{n2}, \quad (\text{A.30d})$$

$$C_{4,1,a} = -b_2 \cdot d_2 \cdot d_{n1}, \quad (\text{A.30e})$$

$$C_{4,1,b} = b_2 \cdot d_2 \cdot d_{n1}, \quad (\text{A.30f})$$

$$C_{4,2,a} = -i \cdot b_2 \cdot d_{n2} / \omega_1, \quad (\text{A.30g})$$

$$C_{4,2,b} = i \cdot d_2 \cdot d_{n2} / \omega_2. \quad (\text{A.30h})$$

